

MUTACIN 1140 AND OCCIDIOFUNGIN: NATURAL PRODUCTS ISOLATED  
FROM BACTERIAL SOURCES AND THEIR POTENTIAL APPLICATIONS AS  
THERAPEUTICS

A Dissertation

by

STEVEN KENNETH LAI HING

Submitted to the Office of Graduate and Professional Studies of  
Texas A&M University  
in partial fulfillment of the requirements for the degree of

DOCTOR OF PHILOSOPHY

Chair of Committee,	James Smith
Committee Members,	Steve Lockless
	James Sacchetti
	Joseph Sorg
Head of Department,	Thomas McKnight

December 2017

Major Subject: Biology

Copyright 2017 Steven Lai Hing

## ABSTRACT

Natural products have long been a template by which science has produced medicines which have saved millions of lives. Bacterial sources have yielded many peptide based drugs which continue to show great value against targets such as Gram-positive and Gram-negative infections. In this work, we will present two natural products yielded from *Burkholderia contaminans* and *Streptococcus mutans* bacteria which have shown great promise against multiple cancer cell lines and Gram-positive infections, respectively. *B. contaminans* produces occidiofungin, a non-ribosomally synthesized cyclic peptide with antifungal properties. Testing against several cancer lines, including ovarian cancer and B-cell lymphoma showed that occidiofungin had efficacy against the cancer lines at a concentration 75 times lower than cytotoxic dosing attempts in mice. *S. mutans* produces mutacin 1140, a lantibiotic product which is ribosomally synthesized and undergoes posttranslational modifications. We have found that *in vitro* dosing of mutacin 1140 in combination with an aminoglycoside, kanamycin against *Staphylococcus aureus* results in a synergistic inhibition effect. Both of these compounds possess great potential as therapeutics.

## DEDICATION

This is dedicated to Steven II and the next Lai Hing generation.

## ACKNOWLEDGEMENTS

I would like to thank my committee members, Dr. Lockless, Dr. Sacchetti, and Dr. Sorg, for their guidance and mentorship throughout the course of this research. Thanks to Dr. Bill Park in the department of Biochemistry who encouraged me to keep going in earning two graduate degrees from Texas A&M.

Dr. James “Leif” Smith was an incredible mentor and committee chair, and was more than I could have hoped for in a supportive PI. He is everything good about academia.

Thanks also goes to my lab mates, Adam Foxfire, Akshaya Ravichandran, Jerome Escano, Mengxin Geng and the Biology department faculty and staff for making my time at Texas A&M University a great experience. Undergraduates William Hedstrom and Travis Madaris greatly contributed to completing the work. Special thanks go to the Biology graduate student advisor, Dr. Arne Lekven and our graduate program coordinator, Jennifer Bradford for their assistance. Thank you to Dr. McKnight for joining my committee.

Finally, thanks to my parents, Dr. Kenneth Lai Hing and Jean Lai Hing for their example and for their encouragement. Thanks to my beautiful wife Ebony and my children for their patience and love. My children are the most important accomplishment of my life.

## CONTRIBUTORS AND FUNDING SOURCES

### **Contributors**

#### *Part 1, faculty committee recognition*

This work was supervised by a dissertation committee consisting of Professor James Smith [advisor], Steve Lockless, and Joseph Sorg of the Department of Biology and Professor James Sacchettini of the Department of Biochemistry.

#### *Part 2, student/collaborator contributions*

The data analysis for Chapter II was provided in part by Professor Smith. The cancer cell experiments depicted in Chapter II were conducted in part by Dr. Kim Loesch of the Department of Biochemistry and Biophysics and were published in 2014. Microscopy for Chapter III was conducted by Dr. Akshaya Ravichandran of the Department of Biology. Mutacin 1140 material in Chapter III was harvested in part by Dr. Jerry Escano of the Smith lab.

All other work conducted for the dissertation was completed by the student independently.

### **Funding Sources**

Graduate study was supported by a teaching fellowship from Texas A&M University Department of Biology. There are no outside funding contributions to acknowledge related to the research and compilation of this document.

## NOMENCLATURE

MIC	Minimum Inhibitory Concentration
Mut1140	mutacin 1140 lantibiotic
Kan	Kanamycin
Strep	Streptomycin
Gent	Gentamycin
Vanc	Vancomycin
CFU	Colony Forming Unit

## TABLE OF CONTENTS

	Page
ABSTRACT .....	ii
DEDICATION .....	iii
ACKNOWLEDGEMENTS .....	iv
CONTRIBUTORS AND FUNDING SOURCES.....	v
NOMENCLATURE.....	vi
TABLE OF CONTENTS .....	vii
LIST OF FIGURES.....	ix
LIST OF TABLES .....	x
CHAPTER I INTRODUCTION: CHALLENGES FACING ANTIBIOTIC TREATMENTS AND ANTIFUNGALS .....	1
Peptide-Based Therapeutics .....	5
Mutacin 1140.....	8
Occidiofungin.....	12
CHAPTER II OCCIDIOFUNGIN AS A CANCER THERAPEUTIC.....	16
Overview .....	16
Introduction .....	17
Methods.....	19
<i>In Vitro</i> Toxicity Screening.....	21
Statistical Analysis .....	22
Results .....	22
CHAPTER III SYNERGISTIC IMPLICATIONS OF A LANTIBIOTIC, MUTACIN 1140 AND AN AMINOGLYCOSIDE, KANAMYCIN IN COMBINATION AGAINST <i>STAPHYLOCOCCUS AUREUS</i> .....	26
Overview .....	26
Introduction .....	27
Methods.....	30

Results .....	35
CHAPTER IV DISCUSSION AND CONCLUSIONS .....	41
Discussion .....	41
REFERENCES .....	49
APPENDIX A .....	62
APPENDIX B .....	78

## LIST OF FIGURES

	Page
Figure 1 Mutacin 1140 and Nisin A structure.....	62
Figure 2 Mutacin 1140 synthesis. ....	63
Figure 3 Structure of lipid II. ....	64
Figure 4 Covalent structure of occidiofungin.....	65
Figure 5 <i>In vitro</i> interaction of occidiofungin with F- and G-actin. ....	66
Figure 6 <i>In vivo</i> visualization of occidiofungin.....	67
Figure 7 Occidiofungin mouse histology slides.....	68
Figure 8 <i>In vitro</i> toxicity screen of occidiofungin.....	69
Figure 9 Synthetic bilayer membranes.....	70
Figure 10 Measuring the fluorescence intensity of carboxyfluorescein release. ....	71
Figure 11 Checkerboard microdilution. ....	72
Figure 12 CFU counts for mutacin 1140 and kanamycin against <i>S. aureus</i> . ....	73
Figure 13 Propidium iodide staining data, <i>S. aureus</i> . ....	74
Figure 14 Propidium iodide staining microscopy positive and negative controls. ....	75
Figure 15 Viability of <i>S. aureus</i> following exposure to antibiotics. ....	76
Figure 16 Checkerboard microdilution assay with vancomycin and kanamycin.....	77

## LIST OF TABLES

	Page
Table 1 Spectrum of activity of occidiofungin.....	78
Table 2 Percent body weight change, serum chemistry and hematology following administration of drug and excipient control.....	79
Table 3 Individual MICs .....	80
Table 4 Combination MICs.....	81

## CHAPTER I

### INTRODUCTION: CHALLENGES FACING ANTIBIOTIC TREATMENTS AND ANTIFUNGALS

Each year, at least 2 million people become infected with bacteria resistant to antibiotics, causing at least 23,000 deaths as a direct result of their infections [1]. Drug resistance has become a major issue with most pathogens, but especially with *Staphylococcus aureus*. There are over 30 types of Staph bacteria, with *Staphylococcus aureus* causing the majority of staph infections. *Methicillin resistant Staphylococcus aureus* (MRSA) infections cost a single 200-bed hospital an average of \$1,779,283 annually [2]. MRSA infections are particularly difficult to treat as several front line drugs are ineffective against it [3]. MRSA also greatly affects those who are already immune compromised [4]. Of particular concern are hospital acquired infections (HAI), as most common HAIs are caused by drug-resistant bacteria, including the previously mentioned MRSA; vancomycin-resistant *Enterococcus faecalis*, (VRE); and *Clostridium difficile*, or C. diff. According to the Centers for Disease Control and Prevention (CDC), HAIs are estimated to occur in approximately 5% of all acute-care hospitalizations [1]. The CDC also estimates that the total medical cost to the U.S. healthcare system from hospital acquired infections is between \$35.7 billion to \$45 billion annually [1]. A recent CDC hospital infection survey with 2,039 hospitals reporting [5] revealed eight pathogen groups accounted for about 80% of reported pathogens. Gram-positive cocci (GPC) cause the

majority of hospital acquired infections with *Staphylococcus aureus* (16%, with more than 50% being methicillin-resistant [MRSA]) and *Enterococcus* species (14%, with vancomycin-resistant enterococci [VRE] accounting for approximately 3.5% of all infections) [5]. Nearly 20% of pathogens reported from all HAIs were the following multidrug-resistant phenotypes: MRSA (8.5%); vancomycin-resistant *Enterococcus* (3%); extended-spectrum cephalosporin-resistant *K. pneumoniae* and *K. oxytoca* (2%), *E. coli* (2%), and *Enterobacter* spp. (2%); and carbapenem-resistant *P. aeruginosa* (2%), *K. pneumoniae* and *K. oxytoca* (<1%) [5].

A brief summary of the current antibiotic classes and their general targets in bacteria is presented here. Cell wall biosynthesis is inhibited by  $\beta$ -lactam containing compounds, such as penicillins and cephalosporins, which inhibit peptidoglycan polymerization by binding penicillin  $\beta$ -lactam ring of penicillin to the enzyme DD-transpeptidase. DD-transpeptidase cannot catalyze formation of these cross-linkages, which causes an imbalance between degradation and cell wall production leading to lysis from an osmotic pressure increase. Polymyxins disrupt the plasma membrane, binding to lipopolysaccharide (LPS) in the outer membrane of Gram-negative bacteria and causing cell death. The plasma membrane sterols of fungi are attacked by polyenes (amphotericin) and imidazoles. Quinolones bind to a bacterial complex of DNA and DNA gyrase, blocking DNA replication. Nitroimidazoles select for anaerobic bacteria due to their ability to reduce metronidazole to its active form. This reduced metronidazole can then covalently binds to DNA, disrupt its structure, inhibiting

bacterial nucleic acid synthesis and resulting in cell death. Rifampin inhibits DNA-dependent RNA polymerase activity. It accomplishes this by forming a stable complex with the enzyme, then suppressing the initiation of RNA synthesis. Aminoglycosides, chloramphenicol, tetracycline, clindamycin, erythromycin, interfere with ribosome function causing the creation of junk peptide fragments and cell death. Lastly, sulfonamides and trimethoprim block the synthesis of the folate required for DNA replication. Sulfonamides stop folic acid synthesis by preventing *para*-aminobenzoic acid (PABA) addition into the folic acid molecule.

While reasons for drug resistance development vary, one reason stems from over prescription and patient dosage regimen incompleteness, giving the bacteria constant association with the compound and developing resistance [6]. Other reasons include biological resistance mechanisms from the bacteria themselves, including the use of multidrug efflux pumps, that is, proteins that cells use to detoxify and export antibiotic compounds from the cell. Pumps seem to play a key role in the emergence of these multidrug resistant (MDR) bacteria [7]. Some resistant bacteria defeat antibiotics by changing critical target sites to avoid recognition by the drug. This has been clinically observed with *Enterococci* altering its cell wall precursor components to decrease successful binding of vancomycin [8]. Of note as well is the lean pipeline of antibiotic candidates [9] against the so called “ESKAPE” pathogens: *Enterococcus faecium*, *Staphylococcus aureus*, *Klebsiella pneumoniae*, *Acinetobacter baumannii*, *Pseudomonas aeruginosa*, and *Enterobacter* species [10].

There is a persistent need not only for novel drug candidates to treat these infections, but also for effective dosing strategies with currently available drugs [9]. Effective combinatorial therapy will allow for a reduction in dose necessary to reach the equivalent (or higher) level of efficacy, which in turn reduces toxicological concerns for drugs currently in the clinic which may still possess efficacy but may cause harmful side effects. An example of such an antibiotic with a high use clinically are the fluoroquinolone class which feature a significantly increased risk of kidney failure in treated patients [11]. The best known examples of fluoroquinolones are Cipro (ciprofloxacin), Levaquin (levofloxacin) and Avelox (moxifloxacin). Combinatorial therapy also provides multiple points of attack for bacteria inhibition, reducing the risk of resistance development in response. In the case of peptide based therapeutics, combinatorial therapy may be especially useful due to limited sourcing and expensive overhead to produce these bacteria synthesized compounds. Current combinatorial therapy strategies include pairing of 1 or more antibiotics into a treatment regimen, which, for the most part is used as a strategy of resistance suppression. Presenting the bacteria with different targets slows the adaptation and resistance mechanism due to multiple mutations being required. Examples of current combinatorial strategies include combining doxycycline and rifampin (for treatment of endocarditis), as well as  $\beta$ -lactam drugs with  $\beta$ -lactamase inhibitors (Clavunate and Amoxicillin) to combat maladies such as sinusitis, pneumonia (usual adult dose calls for 500 mg orally every 8 hours or 875 mg orally every 12 hours) ear infections, bronchitis, urinary tract infections, and

infections of the skin. Combinatorial therapies continue to be a powerful clinical weapon; however, in and of itself, is not enough to completely stem the tide of resistance. New candidate drugs and approaches are needed.

### **Peptide-Based Therapeutics**

Antimicrobial peptides have been studied and analyzed for over 30 years [12, 13].

Peptides are recognized for being highly selective against target bacteria, effective and relatively safe and well tolerated by patients. Side effects are also milder in comparison with other chemi-therapeutics. Currently, there are more than 60 US Food and Drug Administration (FDA)-approved peptide therapeutics on the market; this is expected to grow significantly, with more than 500 therapeutic peptides in preclinical development and approximately 140 peptide drugs currently in clinical trials and [14] [15]. Because of peptide's attractive chemical profile and useful properties, peptides represent a promising starting point for novel drug design [15]. These antibiotics normally are classified as either non-ribosomally synthesized (NRS) or ribosomally synthesized peptides. Examples of NRS peptides include polymyxins, gramicidins, glycopeptides, and bacitracins. Many NRS peptides are produced by bacteria from the genus *Streptomyces* (actinomycin, bacitracin, daptomycin, vancomycin, and teixobactin) and are modified; the ribosomally synthesized peptides are produced by nearly all species. These peptides are normally small (<10 KDa) and of variable length, structure, and sequence [16]. It is this widespread variety and lack of rigid homology which lead to the belief that these peptides were developed over time by multiple species as defense

mechanisms [17]. The significance of naturally produced cationic peptide antibiotics is reflected in their evolutionary origin as inhibitory substances that microbes use against each other [18]. Ribosomally synthesized antibiotic peptides have been isolated from invertebrates and vertebrates, plants, fungi, and bacteria [19]. Most of these peptides may act by selectively disrupting the plasma membrane leading to lysis of the cell [20]. Several peptides have entered clinical trials for treatments such as impetigo (xoma), and diabetic foot ulcers (a thrombin derived peptide used to promote wound healing, chrysalin) [16]. Some of the newest antibiotics to enter the clinic are peptides, such as echinocandins and daptomycin. Echinocandins are a relatively new class of drug which at the time of discovery, represented the first novel class of antifungals in more than 15 years [21]. Their mechanism of action (MOA) is to stop synthesis of  $\beta$ -D-glucan in fungal cell walls. Positive characteristics of echinocandins include rapid fungicidal activity against *Candida* spp. and low toxicity.

Daptomycin is a naturally occurring lipopeptide antibiotic found in the soil saprotroph (extracellular digestion involved in the processing of decayed organic matter) *Streptomyces roseosporus*, isolated by scientists at Eli Lilly from a soil sample from Mount Ararat, Turkey. Daptomycin underwent clinical trials in the late 1980s and early 1990s [22], and is active against multiple categories of Gram-positive bacteria, including MRSA and enterococci [23]. Further studies elucidated that the mechanism of action for daptomycin was that it facilitated formation of membrane distortions. These distortions or membrane patches are able to attract the cell division protein DivIVA

which has been linked with the formation of defects in the membrane and cell morphology changes; it is thought to be essential [24]. This suggests an alteration in the enzyme activity involved in the process of cell wall synthesis that could account for previously described effects of daptomycin on cell wall morphology [24]. Recent success points to the need for new drugs coming from peptide synthesizing sources [15]. However, there is still more that needs to be done to study peptide based compounds for clinical use.

The Smith lab has a research focus on the understanding of the structure and function of natural therapeutic products [25]. This work will provide a foundation for research aimed at understanding their efficacy for use in the treatment and prevention of human and animal diseases and as potential biological control agents in agriculture. The discovery of novel antimicrobials and the study of antimicrobial function have significant relevance towards the development of therapeutics aimed at treating life-threatening diseases [25]. Moreover, much of what we have learned about protein synthesis, DNA replication, enzyme function, and membrane physiology comes from the study of the effect of antimicrobial compounds on the physiology of the target bacteria. The structural and functional characterization of new antimicrobial agents will help provide new insights into cellular processes and membrane physiology, as well as provide a means to rationally design new analogs that target microbial function [25]. The discovery of new enzymes involved in natural product synthesis also offers invaluable information for understanding the complexity of microorganisms and provide tools for

synthetic chemistry applications [25]. Two of the natural product peptides we are focused on are mutacin 1140, a Gram-positive inhibitor which binds lipid II, and occidiofungin, an antifungal compound.

### **Mutacin 1140**

*Streptococcus mutans* JH1140 is a Gram-positive coccus-shaped bacteria naturally occurring in the oral cavity of some individuals; it is a known contributor to tooth decay [26]. It was first discovered by J Kilian Clarke in 1924 [27, 28]. *S. mutans* helps cause tooth decay by creating an acidic environment in the mouth through breaking down sucrose to lactic acid utilizing the enzyme glucansucrase. *S. mutans* produces dextran by using the enzyme dextransucrase and sucrose as a target substrate.

*S. mutans* produces a 22 amino acid post-translationally modified peptide product, named mutacin 1140 (Figure 1). Mutacin 1140 was first discovered by Hillman in 1998 after performing homology analysis of the band resulting from a stab of a spontaneous mutant (JH1140) of JH1000 which produced threefold-elevated amounts of activity [26]. Mutacin 1140 is a bacteriocin (Class 1) showing effective inhibition against Gram-positive bacteria [29]. Mutacin 1140 is classified as a type A lantibiotic, forming unique lanthionine rings in the 1140 structure [29]. Lantibiotics are peptide antibiotics that feature amino acids such as lanthionine or methyllanthionine, as well as unsaturated amino acids dehydroalanine and 2-aminoisobutyric acid. Its antibacterial properties are activated by cleavage of an N-terminal leader [30, 31]. Multiple Gram-positive bacteria

like *Streptomyces* and *Streptococcus* produce lantibiotics in order to eliminate other Gram-positive bacteria competitors [32]. Nisin is of this same class, (perhaps the best known example) and has been used for several decades as a food preservative [33] (Figure 1). The ring structures A and B are conserved between mutacin 1140 and nisin, and are thought to house the region which binds lipid II. Lanthipeptides, (the newer term to replace lantibiotics) have applications as probiotics, therapeutic agents for the treatment of human diseases, and the biosynthetic enzymes have protein chemistry applications. No protein receptor is required for the bactericidal activity of this class of antibiotics, and therefore, resistance is not easily developed via genetic adaptation due to the conservation of the lipid II target. At this point, genetically stable resistant strains to mutacin 1140 have not been found, suggesting that the chemistry and structure of mutacin 1140 may prove valuable as a template for further development of synthetic antibiotics [34].

Mutacin 1140 features amino acids such as methylanthionine (Abu-S-Ala), lanthionine (Ala-S-Ala), didehydroalanine (DHA) and didehydrobuterine (DHB)[35]. Mutacin 1140 is biosynthesized in a series of dehydration steps to its serines (yielding DHA) and threonines (yielding DHB)[36]. It is the formation of a structural ring between the cysteine and either DHA or DHB which forms a lanthionine ring [37]. For these post-translational modifications to occur, several actors forming the biosynthetic gene cluster must be present, including *lanA* (lantibiotic peptide, Figure 2A), *lanB* (dehydratase actor, Figure 2B), *lanC* (which helps facilitate thioether connections and causes cyclization

Figure 2C), decarboxylation by *lanD* (Figure 2D) and *lanT*, a transporter which allows the movement of the peptide [37](Figure 2E). *LanP*, a protease, performs the important step of cleaving the leader sequence, activating the peptide for lipid II sequestration [38] (Figure 2E).

Mutacin 1140's mechanism of action is to sequester and abduct bacterial lipid II, preventing and disrupting cell wall biosynthesis. Lipid II is a peptidoglycan precursor which anchors itself in the bacterial membrane [39] (Figure 3). Its main purpose is to facilitate a transportation network by which peptidoglycan "building blocks" are moved from the cytoplasm to the membrane surface [39]. Lipid II is an essential component for bacterial cell wall integrity. Compounds which attack lipid II can be especially useful due to both the essentiality of lipid II and the low chance of lipid II target resistance development. Lantibiotics have also been shown to disrupt plasma membranes [40]. Previous studies using nisin as a guide elucidated that, unlike nisin, mutacin 1140 does not form a lipid II facilitated pore complex [29]. Further experimentation using fluorescence techniques reveals that mutacin 1140 and nisin competitively bind lipid II. Other current lantibiotics in development include one from Novacta Biosystems Ltd, a type-B lantibiotic-based compound that has antibacterial activity PCT/GB2008/002463). The compound is proposed for use in therapy or prophylaxis for infections caused by *Clostridium difficile* and for treatment of pseudomembranous colitis [18]. Limited work has been done in combining lantibiotics with other therapeutics to assess synergistic or additive effects. Recent literature [41] has appeared which shows

synergistic effects against *S. aureus* when nisin is combined with cinnamaldehyde. Cinnamaldehyde is a well-studied essential oil isolated from cinnamon bark, which previously was reported to exhibit a broad spectrum of antimicrobial activity across a wide range of microorganisms [42]. Another study released this year (2017) shows data supporting synergistic behavior between nisin and citric acid against *S. aureus* and *Listeria monocytogenes* with fractional inhibitory concentration (FIC) ranging from 0.25 to .375 and 0.19 to 0.375 FIC index, respectively [43]. While these studies do show promise combining lantibiotics and compounds with antimicrobial activity, no one has reported studies showing lantibiotics in combination with FDA approved front line or second line antibiotics used clinically. Dosing bacteria with lantibiotics in combination with a secondary antibiotic partner may lead to an improved combinatorial strategy and synergy. I will address this idea further in Chapter III.

Lantibiotics are limited in the sense that they only work against a Gram-positive bacteria. Their ineffectiveness against Gram-negative bacteria occurs due to their large size keeping them from getting through the outer membrane.

An interesting innovation would be conferring lantibiotic activity against Gram-negative bacteria, either by devising a delivery system to bypass the Gram-negative outer cell membrane or by modifying the outer cell membrane itself before dosing to allow passage of the mutacin 1140 inside. Recent work by Vukomanović *et al.* shows some success in this venture; they bound nisin molecules to the surface of gold nano-features and used it effectively against Gram-negative bacteria (*Escherichia coli* and

*Pseudomonas aeruginosa*). They were able to show that this type of structure enables interactions capable of disrupting the outer cell membrane of Gram-negative bacteria [44].

Another research group from Shanghai Jiao Tong University School of Medicine recently demonstrated successful reduction (by three orders of magnitude) of drug-resistant *Escherichia coli* GN102 in a mouse peritoneal cavity using silver core-embedded mesoporous silica nanovehicles in combination with the broad spectrum antibiotic Levofloxacin [45]. The novelty of their nanoparticle delivery system might be adapted to deliver lantibiotics into previously untreatable Gram-negative strains, further opening up the possibilities of lantibiotics easing the pressure on the antibiotic pipeline.

### **Occidiofungin**

In parallel to bacterial infections, fungal infections pose a unique threat to treatment as there is a growing demand for new antifungals given the increasing prevalence of pathogens resistant to current antifungal agents. Fungal infections affect millions of people each year across the world, but especially those who are organ-transplant patients [46]. The use of medically related antifungal drugs in agriculture has resulted in environmental reservoirs for some drug-resistant pathogens [47]. Fungal infections also pose a high chance of relapse which adds another challenge to prognosis [48]. Over the past decade, the development of less toxic drugs, which can be applied safely in a range of patients with various conditions, has contributed to the expansion of antifungal use for

prophylaxis, and empirical and directed therapy, which has in turn led to increased drug resistance [49]. Current treatments for fungal infections include one of three general approaches: by disrupting cell wall biosynthesis (echinocandins), inhibiting ergosterol production (azoles), or binding of ergosterol (polyenes) [50-52]. The emergence of drug resistance to any one drug class severely limits therapy because so few treatment options are available. Multidrug resistance can eliminate treatment options entirely, which has a devastating effect on patient outcome. The only orally available class, the azoles, interacts with several groups of drugs frequently taken by patients in need of antifungal treatment. This can present a situation where therapeutic interference can mitigate the performance of the antifungal.

With the increased presence of resistance against first and second line drugs, fluconazole and echinocandins (anidulafungin, caspofungin, and micafungin); new antifungal candidates are desperately needed to meet the rising challenge of fungal infections. Recent developments now show that there are *Candida* species which are resistant to all known clinically utilized antifungals [53]. According to the CDC, candidemia is the most common blood infection in the United States [54]. Even in cases where resistance is not present, current antifungal treatments lead to abnormal liver function test and have limitations with respect to their spectra of activity and toxicities.

Occidiofungin is a 1200 Da glycolipopeptide compound (Figure 4) purified from the soil bacteria *B. contaminans* MS14 liquid culture [55]. The MS14 strain of *B. contaminans* was isolated from soil and was discovered by its ability to inhibit brown patch lawn

disease [56, 57]. *Burkholderia contaminans* is a Gram-negative, non-sporulating, rod-shaped, motile, aerobic bacteria which has received attention due to their infections being difficult to treat (normally requiring combinations of antibiotics) due to their resistance to antibiotics. Members of the bacteria *Burkholderia* exist naturally in environments such as water, soil, and the plant-root interface of crop plants[58]. Some *Burkholderia* strains show high efficacy in killing fungal diseases in crops and form a potent tool for plant disease management [59]. Unfortunately, the use of *Burkholderia* strains is not currently allowed due to the difficulty differentiating these useful strains from the pathogenic strains associated with the human disease cystic fibrosis [55, 60]. Recent work from our lab has taken steps towards addressing this issue in classifying pathogenic strains, by performing comparative genome-wide analysis and sequencing on *B. contaminans* MS14. The comparison study revealed that the *Burkholderia* species genome show considerable diversity, and was different from the compared pathogenic strains in several key ways, namely in the absence of virulence-associated gene loci and the presence of multiple antimicrobial activity-related genes [61]. The gene cluster which was predicted to be responsible for the production of occidiofungin, the *ocf* cluster, was characterized and of the 16 open reading frames (ORFs) that are present in the cluster, five (ORF5, 6, 7, 9 and 11) were predicted to be NRPS or NRPS-PKS. ORFs 4, 12, 13, 14 and 15 are involved in the modification of occidiofungin [62]. AmbR1 and AmbR2 regulate the production of occidiofungin[63]. Occidiofungin has potent fungicidal activity against multiple fungi including *Fusarium spp.*, *Cryptococcus neoformans*, as well as *Candida albicans*. The mechanism of cell death against yeast has

been shown to be apoptotic [64]. MIC values for occidiofungin versus industry used drugs such as echinocandins and amphotericin B are comparable (submicromolar to micromolar) (Table 1). Previous mouse studies [56] showed that high doses did not result in mortality. Recent work from our lab [62] points to actin being the target of occidiofungin by several methods, including confocal microscopy and pull down assays (Figure 5). F- or G-actin incubated with the wild type occidiofungin and DMSO was used as a control for potential non-specific interaction of actin with the agarose beads. As shown in Figure 5, the biotinylation of alkyne-OF was required for the binding of F- or G- actin to the streptavidin beads (Lane 5 and 8). Actin was not detected in the control lanes (lanes 6, 7, 9 and 10). The eluant from the biotinylated alkyne-OF had a single band at approximately 42 kDa which is the expected size for actin. Therefore, the affinity purification assays done with F- or G-actin confirmed that occidiofungin binds to actin. Similar studies in *Schizosaccharomyces pombe* demonstrated localization of occidiofungin near the poles of the cells and in areas which are well-documented regions for actin patches [65] (Figure 6). Actin is a group of proteins that form filamentous structures (microfilaments). They are present in most eukaryotic cells. Actin plays a key role during metastasis of cancer cells in transit and growth at new sites, as well as cell motility. For this reason, it is a high value target for cancer therapeutics and informs our interest in investigating whether occidiofungin might possess cancer treatment properties independent of its known antifungal applications.

## CHAPTER II

### OCCIDIOFUNGIN AS A CANCER THERAPEUTIC\*

#### **Overview**

Occidiofungin, a glyco-lipopeptide obtained from the liquid culture of *Burkholderia contaminans* MS14, has been identified as a novel fungicide. The natural product was shown to have a minimal amount of toxicity in a previous mouse toxicity study following intraperitoneal and subcutaneous administration. In this study, the toxicity of occidiofungin was evaluated following a 5 mg/kg intravenous tail vein injection. In addition, the toxicity of occidiofungin was evaluated against human fibroblast and cancer cell lines. Weight loss was the most significant observation following intravenous administration of occidiofungin. Histology, hematology, and blood serum chemistry did not reveal any significant signs of toxicity. The activity observed in the *in vitro* cytotoxicity assay against the cancer cell lines was all below 75 nM of occidiofungin. To date, the potency of occidiofungin against these cancer cell lines is greater than any activity observed against fungi. The findings in this study support the need to further evaluate occidiofungin's chemotherapeutic potential.

---

\*Reprinted with permission from “Toxicological Evaluation of Occidiofungin against Mice and Human Cancer Cell Lines” by Steven Lai Hing, Akshaya Ravichandran, Jerome Escano, Leif Smith *Pharmacology & Pharmacy*, Vol.5 No.11, 1085-1093 Copyright 2014 by Steven Lai Hing

## **Introduction**

Occidiofungin is a compound purified from liquid culture of *Burkholderia contaminans* MS14 [57, 64, 66-71]. The compound is a non-ribosomally synthesized cyclic peptide, composed of eight amino acids, having a base mass of 1200 Da (Figure 2). An eighteen carbon fatty amino acid with a xylose sugar attached was identified in the compound, along with non proteinogenic amino acids 2, 4-diaminobutyric acid (DABA), and beta hydroxyl tyrosine and asparagine. Biological activity assays demonstrated its potent antifungal properties against a broad spectrum of plant and animal fungal pathogens [57, 64, 66, 71].

The strong inhibitory effect of occidiofungin on *Pythium* spp., which does not express ergosterol in the cell membrane and chitin in the cell wall, suggests that inhibition of ergosterol or chitin biosynthesis is not a major component of occidiofungin activity. The inhibitory activity of occidiofungin on *Fusarium* spp. and *Cryptococcus neoformans*, which are resistant to echinocandins, suggests a new antifungal mechanism may be involved [57, 69]. Pharmacodynamic experiments revealed that occidiofungin's fungicidal activity against *Candida albicans* is more rapid than the fungicidal activity reported for the echinocandin antifungal caspofungin [72, 73]. Potent fungicidal activity was observed against *Candida albicans* following a short term exposure to occidiofungin for only one hour, suggesting that occidiofungin has a strong interaction with a cellular target [66]. Furthermore, the mechanism of cell death in yeast has been determined to be apoptotic [64]. These results indicate that occidiofungin is distinctive from the four existing classes

of clinically used antifungal drugs and that occidiofungin's potential as a therapeutic agent warrants further investigation. The  $TC_{50}$  (toxic concentration resulting in 50% cell death) against mouse fibroblasts was 3  $\mu$ M, which is similar to the MICs against *Candida* species [66]. Minimum inhibitory concentrations (MICs) of occidiofungin against *Candida* species are submicromolar to micromolar, which is similar in activity to echinocandins and amphotericin B [66, 72, 73]. The target for occidiofungin is presumably present in most eukaryotic cells, given that the activity of occidiofungin against mouse fibroblasts and *Candida* species is only a few folds different.

Before testing the efficacy of occidiofungin in an animal model or in humans, it is necessary to determine its toxicological profile. Substantial toxicity at doses expected to be required for antifungal efficacy would preclude further development of this compound as a therapeutic agent. Interestingly, a mouse toxicity study showed that doses higher than those commonly used to treat fungal infections did not result in mortality [74]. Furthermore, a dose administered intraperitoneally as high as 20 mg/kg resulted in no negative gross or microscopic findings in the liver or kidneys. Hematology and serum biochemistry tests also revealed that occidiofungin does not significantly alter organ function [74]. One possibility for the lack of observed organ specific toxicity in the previous mouse study is that occidiofungin did not absorb well into the circulatory system and that the lack of absorption was the reason for the lack of organ specific toxicity observed.

Considering that at the time of this work the target for the observed activity of occidiofungin was still unknown (actin) and that *in vitro* toxicity was seen in both fungal and mouse fibroblasts, the aim of this study was to evaluate the toxicity of occidiofungin in mice following intravenous administration along with its cytotoxicity against human cell lines. We found that cancer cell lines are hypersensitive to occidiofungin and that intravenous administration is well tolerated in the mouse model. Overall, our studies support the need for additional studies to evaluate occidiofungin's chemotherapeutic potential.

## **Methods**

***Mice.*** Female BALB/c mice at age of 6 – 8 weeks old were used. Female mice were used instead of male mice, given that male mice generally exhibit more aggressive behavior. These mice were purchased from Harlan and allowed to acclimate at least 2 weeks after arrival. They were housed on a 12 hour light-dark cycle in a temperature and humidity controlled animal facility that is accredited by the American Association for Accreditation of Laboratory Animal Care. Animal care and use were in accord with NIH Guidelines and Texas A&M University regulations. Protocols used for the mice models were done in accordance to the methods reported by Luster et al [75].

***Single Dose Toxicity Study [75].*** Occidiofungin was produced as previously described and aliquoted and lyophilized into 100 µg quantities in 1.8 mL centrifuge tubes. Solubility of occidiofungin in aqueous buffers is relatively low. Mice (5 mice per group) were given

occidiofungin dissolved in 1.5% hydroxy propyl-beta-cyclodextrin suspended in phosphate buffered saline (PBS). Hydroxy propyl-beta-cyclodextrin has been used extensively in pre-clinical drug testing with little or no indication of meaningful effects [76]. Spectrometric inspection at O.D.<sub>600</sub> following addition of vehicle to the purified dried drug had negligible absorbance difference to vehicle without drug, suggesting that the drug went into solution. For the experiments, occidiofungin was administered by intravenous (i.v.) injection into the tail vein at a single dose at 5 mg/kg of body weight. The excipient control in each experiment matched the vehicle. Body weight and clinical signs (movement, posture, skin lesions, appearance of fur indicating normal grooming, and behaviors) were recorded following administration at one, four, eight, sixteen, and twenty-four hours. Necropsies were performed at 24 hours following administration of occidiofungin.

***Measurement of Toxicological Parameters [75].*** Blood and tissue samples from animals dosed at 5 mg/kg of body weight with occidiofungin in 1.5% hydroxy propyl-beta-cyclodextrin suspended in PBS were taken 24 hours following excipient or drug administration. Mice were anesthetized with isoflurane. Blood was then taken from the retroorbital plexus or heart puncture for serum biochemistry assays (alkaline phosphatase, alanine aminotransferase, aspartate aminotransferase, albumin, and blood urea nitrogen) and hematology (white blood cell count and white blood cell differentiation). Body weight was measured immediately before treatment and 24 hours later before the mice were fully anesthetized and fixed in 10% neutral buffered formalin. Histological examination was

performed on a portion of each organ by using routine paraffin embedding technique and staining with hematoxylin and eosin (H & E) [77]. All the sections were examined under light microscopy for pathological changes by a co-author of this paper, who is a board certified veterinary pathologist (J. C.).

### ***In Vitro* Toxicity Screening**

Cancer cell lines, OVCAR8 (Center for Cancer Research (OVAR.8; Sample ID 25)), SW1088 (ATCC-HTB-12), and Toledo (ATCC CRL-2631), and normal human neonatal dermal fibroblasts (ATCC-PCS-201-010) cell line were passaged and prepped as previously described [78-80]. OVCAR8, SW1088, and Toledo2631 are an ovarian, brain, and B-cell lymphoma cancer cell lines, respectively. Cell counts per plate were calculated to be approximately 50,000 cells/mL. A 10X stock solution of occidiofungin was prepared at 65  $\mu$ M concentration in 10% dimethyl sulfoxide (DMSO). Two-fold serial dilutions on a 96 well plate were set up in triplicate with starting concentration of 6.5  $\mu$ M and a final concentration of 3 nM. Bortezomib was used as a comparator for toxicity against human fibroblast and was serially diluted two-fold starting at a concentration of 5  $\mu$ M and ending at 2.5 nM. Bortezomib is used clinically against myeloma and lymphoma cancers in patients' refractory against other chemotherapeutics [81, 82]. The plates were then incubated at 37°C in 5% CO<sub>2</sub> for 48 hours. After 48 hours, cell viability was monitored using CellTiter-Blue (Promega) cell viability assay by measuring the fluorescence emission of a redox activated dye (579<sub>EX</sub>/584<sub>EM</sub>) using a POLARstar Omega microplate reader (BMG Labtech).

## **Statistical Analysis**

Body weight, body weight change, organ weight, serum chemistry and hematology data were analyzed by T-test or two way ANOVA followed by Bonferroni post-test using Prism GraphPad software (San Diego, CA). All the analyses were two-sided, with  $p < 0.05$  considered statistically significant.

## **Results**

*Anatomic and Clinical Pathology.* Results shown in Table 2 indicate the change in body weight following a single 5 mg/kg i.v. dose after 24 hours. Excipient treated mice body weight ranged between an 8% to 13% body weight gain after treatment and had a 9.6% average increase in body weight. Occidiofungin treated mice weight ranged between a 0% to a 21% body weight loss after treatment and had an average weight loss of 6.2%.

A consistent behavioral response was observed at 1 hour and to a lesser extent at 4 hours post i.v. administration, in which the mice were more lethargic than excipient treated mice and had ruffled fur. They were responsive to touch, but would move slower than excipient treated mice. Treatment was not associated with more typical rodent behaviors associated with severe pain (e.g., writhing, vocalization, or lack of spontaneous locomotion). No other behavioral signs were observed. Mice behavior appeared to be normal by 8, 16, and 24 hour post injection.

Generally, no macroscopic findings were observed by histological examination. No observable differences were present in the microscopic cell morphology or macroscopic

tissue morphology of esophagus, stomach, small intestine, colon, liver, pancreas, spleen, kidneys, lungs, heart and brain (Figure 7). Albumin and blood urea nitrogen (BUN) tests were similar for occidiofungin treated and excipient treated mice (Table 2). These blood tests are indicative of normal kidney and to some extent liver function. In addition, alkaline phosphatase (ALP) tests were similar between drug and excipient treated mice (Table 1). These results indicate normal liver and bone cell function. Normally aspartate amino transferase (AST) and alanine aminotransferase (ALT) tests are performed in combination with ALP to assess liver function. Elevated levels of AST and ALT do suggest heart or liver damage, but do not necessarily indicate severe organ damage. Generally a ratio of AST to ALT less than one is indicative of liver damage. The ratio in all treated mice was greater than one, suggesting that the liver is not damaged. AST values ranged from 177 to 1528 (U/l) with a mean value of 765 (U/l) and the ALT values ranged from 144 to 1273 (U/l) with a mean value of 521 (U/l) (Table 2). Given the variability in AST and ALT levels in treated mice, only the ALT levels were statistically significant.

White blood cell (WBC) counts were not statistically different between treated and untreated mice. This suggests that occidiofungin i.v. administration at 5 mg/kg had no cytotoxicological effect on blood cells or bone marrow. The absence of elevated levels further suggests normal spleen function. The percentage of neutrophils was statistically different in drug and excipient treated mice, while the percentages of lymphocytes were not statistically different (Table 2). The data does suggest an increase in the ratio of neutrophils to lymphocytes, which is indicative of an innate immune response to the drug.

However, additional mice and dosing regimens will need to be done to determine if this is a genuine response. Lastly, there was no statistical difference in platelet counts between drug and excipient treated mice, suggesting that occidiofungin does not affect platelet production by the bone marrow or destroy circulating platelets.

In summary, there was no clear evidence for organ specific histological effects of occidiofungin. There were no apparent undesirable effects observed in the serum clinical chemistry and hematology parameters that would preclude additional animal testing of the compound.

***Cytotoxic Activity of Occidiofungin on Human Cell Lines.*** Bortezomib is a proteasome inhibitor that has been accepted by the medical community as a potent anticancer drug. It is a potent inhibitor of multiple myeloma and pancreatic tumor growth [81, 82]. The proteasome is a multi-catalytic, multi-subunit protease complex that is responsible for the ubiquitin-dependent turnover of cellular proteins [82-84]. Interference with the normal function of the proteasome by bortezomib affects cellular pathways that can interfere with transcription, release of cytokines, interfere with DNA repair machinery, and the activation of signalling kinase pathways that alters a cohort of cellular responses [83-86]. These activities are exacerbated in multiple cancers. A typical LD50 value for bortezomib is between 20 and 50 nM, while its toxicity is in normal cells with lower metabolism is typically in the micromolar range [83, 87]. The activity of bortezomib was compared to the activity of occidiofungin against human fibroblasts. The activity of occidiofungin was

approximately eight-fold higher than that of bortezomib against the human fibroblast cell line used in this study (Figure 8).

These results suggest that the biological target of occidiofungin or the cellular effect due to the interaction with the target is augmented by the cellular physiology of the human cancer cell lines.

## CHAPTER III

### SYNERGISTIC IMPLICATIONS OF A LANTIBIOTIC, MUTACIN 1140 AND AN AMINOGLYCOSIDE, KANAMYCIN IN COMBINATION AGAINST *STAPHYLOCOCCUS AUREUS*

#### **Overview**

*Streptococcus mutans* JH1140 is a strain of bacteria which produces a lantibiotic named mutacin 1140. Mutacin 1140 has been shown to be effective at inhibiting Gram-positive bacteria associated with *Staphylococcus aureus* and *Streptococcus pneumoniae* infections. Mutacin 1140 is a ribosomally synthesized peptide antibiotic that undergoes extensive posttranslational modifications (PTM). Microdilution plate assays show that when combined, mutacin 1140 and kanamycin, an aminoglycoside, displays synergistic behavior against *S. aureus*. The proposed mechanism of action for this synergistic behavior is different than kanamycin's (30S ribosome action) individual mechanism of action, pointing to a cooperative membrane perturbation combined with cell wall inhibition. Confocal microscopy of propidium iodide stained cells treated with a combination of mutacin 1140 and kanamycin alluded to the possibility that combined, the effect of bacterial cell death is faster than individually against both *Staphylococcus aureus* and methicillin-resistant *Staphylococcus aureus* (MRSA). Additional studies, determining cell viability at 30 minutes by counting the colony forming units further showed that the combination of the antibiotics is more effective at inhibiting a clinically relevant bacterium *Staphylococcus aureus*.

## Introduction

Mutacin 1140 [38] was first isolated from *Streptococcus mutans* JH1140. This peptide shows the characteristic lanthionine structures found in this class of antibiotics called lantibiotics [88]. The presence of a lanthionine rings is common to all lantibiotics with nisin being the most studied representative lantibiotic. The mechanism of action of mutacin 1140 is to sequester lipid II, preventing proper cell wall synthesis leading to a growth inhibitory effect on select Gram-positive bacteria. In other lantibiotics, as in the case of nisin, the lipid II-lantibiotic complex form a pore structure in the cell wall; however mutacin 1140 does not exhibit these pore forming properties in 1,2-dioleoyl-sn-glycero-3-phosphocholine (DOPC) vesicles or against a tested strain of *Streptococcus rattus* [40]. Previous work [29] with bacteria mimetic vesicles containing 50 mM quenched carboxyfluorescein that were treated with submicromolar concentrations of mutacin 1140 (Figures 9 & 10) caused vesicles to lyse and release the carboxyfluorescein. The detection of the carboxyfluorescein release points to an alternative membrane disruptive activity of mutacin 1140. Additional studies showed that increasing the amount of the negatively charged lipid DOPG or the creation of a negatively charged membrane potential caused an increase in release of carboxyfluorescein. Up until the year 2000, research in the field implicated membrane perturbation as the mechanism of action for mutacin 1140 and other type AI lantibiotics and was later documented that lipid II sequestration was the primary basis for its mechanism of action.

Kanamycin is an aminoglycoside bactericidal antibiotic isolated from the bacterium *Streptomyces kanamyceticus* [89]. Aminoglycosides show very little effectiveness against fungi, anaerobic bacteria, and viruses. Aminoglycosides are effective primarily in infections involving aerobic, Gram-negative bacteria. In addition, some mycobacteria, including the bacteria that cause tuberculosis, are susceptible to aminoglycosides.

Kanamycin was discovered in 1957 by researchers in the National Institute of Health of Tokyo, Japan. It was isolated from a soil sample [90] and extracted with a cation exchange resin. It's most used form is as kanamycin sulfate. It targets the 30S subunit of the ribosome, causing mistranslation of and indirectly inhibiting the process of protein synthesis translocation [91, 92]. This leads to a buildup of mistranslated proteins unable to perform their cellular function and the death of currently dividing cells [91].

Kanamycin is currently used as a second line treatment for hospital acquired infections, such as sepsis and urinary tract infections as well as its main use against tuberculosis [93] and is currently placed on the World Health Organization's List of Essential Medicines. Its classification on the list states that it is a backup second-line drug for the treatment of multidrug-resistant tuberculosis (MDR-TB).

*S. aureus* is a Gram-positive bacteria normally found on the epidermis where moisture is present, as well as in the respiratory tract. Skin infections, food poisoning, and Abscesses are commonly caused by *S. aureus*. *Staphylococcus* was first identified by surgeon Sir Alexander Ogston in pus from a surgical abscess in 1880 [94]. While not

always pathogenic, pathogenic strains of *S. aureus* produce toxins which target cell surface receptors and cause apoptosis, and is linked or has been identified as a cause of several illnesses, including endocarditis, sepsis, meningitis, and pneumonia [95]. *S. aureus* exhibits resistance in multiple ways dependent on the antibiotic challenge it faces. For penicillin, *S. aureus* uses penicillinase, an enzyme which cleaves the  $\beta$ -lactam ring, causing penicillin to be ineffective. Glycopeptide resistance occurs by altering the peptidoglycan to which vancomycin will not be able to bind. Aminoglycoside resistance in *S. aureus* normally exhibits one of three generally accepted ways: mutations to the ribosome itself, modifying enzymes for aminoglycosides, and active pumping of the drug out of the bacteria by efflux.

In this study, we evaluated the use of the lantibiotic mutacin 1140 in combination with a select panel of antibiotics. Synergy was confirmed between mutacin 1140 and the aminoglycoside kanamycin through microdilution studies, dose dependent kill curves, and colony forming unit (CFU) counts. Furthermore, propidium iodide (PI) staining and confocal microscopy shows that disruption of the bacterial membrane is faster in dose combination of mutacin 1140 and kanamycin than individually against both *Staphylococcus aureus* and *methicillin-resistant Staphylococcus aureus* (MRSA).

In addition, several substitutions were made to determine if the synergistic behavior was class specific or only observed with single class of compounds. Tetracycline was substituted for kanamycin in combination with mutacin 1140 and nisin was substituted for mutacin 1140 in combination with kanamycin; both substitutions resulted in the loss

of the synergistic effects. However, there were improvements in inhibition with these antibiotic combinations, suggesting that the synergistic behavior observed between mutacin 1140 and kanamycin may have more to do with the class of antibiotics and not just these individual antibiotics.

## **Methods**

**Chemicals.** Mutacin 1140 was produced and purified as previously described [26].

Other reagents were purchased from VWR and were of ACS grade purity unless stated otherwise.

**Media and Drug Preparation.** THyex-M17 media (500 mL) containing 400 mL water, 15 grams of Todd Hewitt media powder (BD), and 1.5 grams yeast extract (BD) was volume adjusted to 500 mL with dH<sub>2</sub>O, sterilized at 121 °C for 35 minutes, and allowed to cool to room temperature. THyex agar plates were made in a similar method (7.5 grams agarose (BD) added) and poured while still warm under sterile conditions. These plates were then stored at 4 °C until use. As a precaution, the plates were preincubated before streaking to ensure no contamination was present. Antibiotics were not added to the agar. Antibiotic stocks (as well as all other drugs tested) were measured in 100 mg/mL concentration aliquots in water and diluted accordingly to the concentrations needed for each respective assay. New solutions were made for each day's experiments and stored at -20 °C.

***S. aureus Growth Parameters.*** *Staphylococcus aureus* was streaked on a solid agar THyex plate and allowed to grow overnight in an incubator set to 37 °C. A 5 mL THyex liquid culture was started using a single colony from a the overnight plate, and spun on a wheel at 37 °C until its optical density (OD) reached (OD 0.11-0.13) to meet the CLSI threshold of McFarland Standard of 0.5. The culture was then diluted 1:300 and then dosed with the drugs. Final *S. aureus* cell counts per well for starting concentration were at minimum 5x10<sup>5</sup> cells. All OD readings were taken by a Bio-Rad SmartSpec plus spectrophotometer.

***Microdilution Assay.*** Microdilution plate based assays were performed following a modified CLSI protocol. Bioassays were done using a 96-well plate with a final volume of 200 µL per well. Each assay was performed in triplicate wells. The 96-well plates were shaken at 170 RPM and allowed to grow at 37 °C; they were read at multiple time points by a spectrometer (Bio-Rad Xmark) in order to generate growth curves, as well as directly observed visually to see if the well showed growth or a change in opacity. Any growth present in the well that was visually distinguished was classified as ineffective antibiotic treatment. MICs were determined to be the highest concentration of antibiotic that inhibited the growth of the bacteria. As a follow up, plates were also stained with cell titer blue (promega G808A) which is a homogeneous, fluorometric method for visually confirming inhibition or growth of bacteria in multiwell plates. It uses the indicator dye resazurin to determine the metabolic capability of bacterial cells—an indicator of overall cell viability [96]. Active cells retain the ability to convert resazurin into resorufin, which

appears as a pink color and is highly fluorescent. Wells which stain blue and stay blue are not metabolically active and are probably dead.

**Checkerboard Assay.** The combination effect of mutacin 1140 and kanamycin was determined by checkerboard assay [97] (Figure 11) and evaluated algebraically based on the fractional inhibitor concentration indices (FICs) . A total of 200  $\mu$ L THyex media was distributed into each well of the 96-well plates. The first antibiotic (mutacin 1140) of the combination was serially diluted along the X-axis and upwards, while the second drug (kanamycin) was diluted along the Y-axis and to the right, where it shared a well with the respective vertical concentration of mutacin 1140. Each well was inoculated with  $5 \times 10^5$  cells *Staphylococcus aureus* grown as previously described, and the plates were incubated at 37°C for 24 hours under aerobic conditions. One well with no antibiotic was used as a positive growth control on each plate. Plates were read for visual turbidity, and results were recorded after 24 h of incubation at 37°C in an enclosed shaker at 170 RPM (Thermo Scientific MaxQ 4000).

***Kill Curves and CFU Counts.*** *Staphylococcus aureus* was grown as previously described in 10mL volumes, and then incubated with varying doses (4X, 2X, 1X, and 0.5X MIC) of the aminoglycoside kanamycin, and the lantibiotic mutacin 1140. The volumes were then shaken together at 170 revolutions per minute (RPM) in combination over 24 hours at 37 °C in a Falcon™ 50 mL conical tube. During that 24 hours they were then tested using the CFU count method; 100 µL of cell suspension from serially diluted cultures were plated on THyex agar and allowed to grow overnight at 37 °C. Several time points (0,2,4,8,12,20 hrs.) leading up to the final 24 hour time point were tested for colony forming units (CFUs). Colonies were then counted, both by hand independently by more than one lab member and assessed using OpenCFU software [98], allowing a reproducible extrapolation of the bacterial cell count at each time point in the presence, absence, and combination of the drugs. Plates with lawns or more than 300 colonies or less than 30 colonies were excluded and a dilution plate within this colony range was counted (Figure 12).

***Staining and Microscopy.*** A culture of *Staphylococcus aureus* was grown to a concentration high enough to yield a visible pellet when spun down. This was accomplished by inoculating 20 mL with one colony overnight, letting it grow up, and then taking 1 µL of that starter culture into a 10 mL experiment culture the following morning and monitoring its growth until it reaches an OD of 0.3. One mL aliquots were taken from the 10 mL experiment culture and placed in separate Eppendorf tubes and

spun down at 6500 RPM (3968 rcf) for 1 minute 30 seconds. 20  $\mu$ L propidium iodide (ThermoFisher P3566) was diluted into 2 mL of Annexin-V-FLUOS incubation buffer and then added in 200  $\mu$ L quantities to each sample. The pellets were then resuspended with the 200  $\mu$ L propidium iodide totaling 10  $\mu$ g/mL final concentrations in each Eppendorf. The tubes were then treated with doses of kanamycin and mutacin 1140 both individually and together. Propidium iodide stain (PI) is a widely used red-fluorescent nuclear and chromosome counterstain. Since propidium iodide is not permeant to live cells, it is also commonly used to detect dead cells in a population. Visual confirmation of red staining on microscopy indicates that the bacterial cell membrane has been compromised to the extent that the stain was allowed access to the nucleic acids. PI binds to DNA by inserting between the DNA bases without sequence preference. In aqueous solution, the dye has excitation/emission measurements of 493/636 nm. Once the dye is bound, its fluorescence is enhanced 20- to 30-fold, the fluorescence excitation maximum is shifted  $\sim$ 30–40 nm to and the fluorescence emission maximum is shifted  $\sim$ 15 nm, resulting in an excitation maximum at 535 nm and fluorescence emission maximum at 617 nm [99].

After 1 minute, 5 minutes, and 10 minutes elapsed for each respective sample, these PI-incubated tubes were centrifuged at 6500 RPM on an Eppendorf 5424 microcentrifuge, decanted and then washed with 200  $\mu$ L phosphate buffered saline (PBS) adjusted to 7.2 PH. They were then immediately fixed with a 3.7% formaldehyde solution (EMD FX0410-5). A 30  $\mu$ L volume of the fixed cells was pipetted from each sample onto a

separate glass slide with the P100 pipette tip snipped to avoid cell shearing, covered with a glass coverslip, and confocal microscopy images were then taken on an Olympus IX81 microscope. Figure 11 shows positive (1% Triton at 2 minutes exposure) and negative (no drug added) controls. Several images with multiple fields of view were taken, both in the presence and absence of the overlaid fluorescence filter. Cell counts were assessed using Olympus Micro FV10-ASW viewer software. Counts consisted of cells which glowed red under filter as well as the overall total number of cells in a field of view. By this method we were able to quantitate a percentage of cells in each view which featured compromised membranes compared to the total count of cells present.

## **Results**

Lantibiotics have not yet been developed successfully as a clinical treatment option for bacterial infections. This is in part due to the difficulty in their production and in part to their short half-life in blood. Furthermore, lantibiotics have a limited spectrum of activity in that they are only effective at treating Gram-positive bacterial infections. Whether lantibiotics will ever find their place in a clinical setting is unknown, and they may continue to be an academic exercise. The current approach for the clinical development of lantibiotics may be wrong and their place in the clinic may be in their use in combination with other approved antimicrobial drugs. Table 3 shows the beginning of our work of determining individual MICs against two strains of *S. aureus* and our activity indicator strain *M. luteus*. The short list of antibiotics target many of the clinically important targets, *i.e.* cell wall synthesis, membrane perturbation, and

translation. Table 2 results were determined with microdilution assays consisting of 3+ rows of serially diluted compounds individually plated against different bacteria strains. Microdilution assay results consistently showed rows of wells of both mutacin 1140 and kanamycin at MIC values individually able to clear the *S. aureus* bacteria from the well. Staining with cell titer blue confirmed that those wells with MIC concentrations had inhibited growth (they stayed blue). Microdilution assays also were used to assess the other antibiotics tested and form the basis for the individual MIC data shown in Table 3.

Once we determined that the clinically relevant *S. aureus* was sensitive to the selected antibiotics, we further characterized their use in combination with mutacin 1140. The Gram-negative membrane disruptor (polymyxin B) is generally not effective against Gram-positive bacteria due to the thickness of their cell wall. We did test whether the combination of polymyxin B in combination with mutacin 1140 against the Gram negative bacteria *Erwinia amylovora* and *Escherichia coli* was more effective in a checkerboard assay, but there was no benefit to the addition of mutacin 1140 in these assays (data not shown). However, synergistic activity was observed between the aminoglycoside kanamycin and mutacin 1140 in the checkerboard assay (Figure 11). Individually, mutacin 1140 and kanamycin had low micromolar MICs of 6.25 and 3.25  $\mu\text{g/mL}$ , respectively. In the checkerboard assay, the effective MIC of each dropped by at least 4-fold when used in combination. Both mutacin 1140 and kanamycin MIC decreased to 0.78  $\mu\text{g/mL}$ , an 8-fold decrease for mutacin 1140 and a 4-fold decrease for kanamycin (Figure 11). Thus, the checkerboard assay results showed synergy between

mutacin 1140 and kanamycin. This effect lasted past the 24 hour mark for assessing the plates after shaking and was reproducible with different stocks of mutacin 1140 and kanamycin (data not shown).

The fractional inhibitory concentration (FIC) index ( $\epsilon$ FIC) was calculated as follows:

$$\epsilon\text{FIC} = \text{FIC A} + \text{FIC B}$$

Where FIC A is the MIC of the combination/MIC of drug A alone, and FIC B is the MIC of the combination/MIC of drug B alone. The threshold for synergy is met when the  $\epsilon$ FIC is  $<0.5$ , indifferent when the  $\epsilon$ FIC is  $>0.5$  to  $<2$ , and antagonistic when the  $\epsilon$ FIC is  $>2$  (Figure 11). FIC calculations for mutacin 1140 and kanamycin gave a value of .3748, well below the 0.5 synergy threshold. Mathematically each compound must have at least a four-fold reduction in MIC to reach the synergistic threshold (Figure 11).

Additional studies were done to determine whether the observed synergy was compound specific or whether the observation could be observed between antibiotics from the same class of compounds (Table 4). Instead of mutacin 1140, we substituted nisin, another lantibiotic with a similar MOA targeting lipid II. The  $\epsilon$ FIC for the combination of nisin and kanamycin was 0.70. It did not meet the cutoff score for synergy, but there was a two-fold decrease and a four-fold decrease in the MIC for nisin and kanamycin when used in combination. There was no improvement in the activity of nisin when used in combination with another aminoglycoside gentamycin. Of interest was a 32-fold reduction in activity of mutacin 1140 when used in combination with

gentamycin, but this didn't meet the criteria for synergy given that there was only a twofold reduction in the activity of gentamycin. Mutacin 1140 was tested in combination with another aminoglycoside, streptomycin and other ribosomal inhibitors spectinomycin and tetracycline, but there was no change in the respective antibiotic inhibitory values. Of note is the observed antagonistic behavior between vancomycin and mutacin 1140 (Table 4). A possible reason for this observed behavior is that mutacin 1140 and vancomycin share the same target in lipid II, albeit focusing on distinct binding sites. Perhaps the binding mechanisms of these two compounds restrict access to the other in competition for lipid II

To further elaborate on our observed synergy we performed CFU kill curves with mutacin 1140 and kanamycin and determined that the result was reproducible in this assay as well. CFU count results (Figure 12) corroborated the observed microdilution assays. The combination of kanamycin and mutacin 1140 at 0.5 MIC concentration killed *S. aureus* faster and prevented substantial regrowth at the 24 hour time point. Sub MIC concentrations of mutacin 1140 and kanamycin repeatedly kept the test culture visibly clear for 24 hours, while simultaneously yielding no visible colony forming units on the corresponding time point agar plates (outside of time zero). In comparison, the no drug control as well as the sub MIC individual volumes plated a lawn of colonies. The media only control consistently did not show any colony forming units, demonstrating that no contamination was present. CFU's also were visibly compared to model examples of *S. aureus* morphology and were confirmed by Gram-staining and

light microscopy (Olympus) during the preliminary portions of the experiment to be the expected Gram-positive bacterium.

Improvement in the activity of mutacin 1140 were only observed when used in combination with the aminoglycosides kanamycin and gentamycin and was not observed with other translational inhibitors. It is possible that the synergy is due to the alternative mechanism of action of aminoglycosides, in which they disrupt membrane integrity. This is presumed to be attributed to the mistranslation of products into the cell membrane by the ribosomes associated with the inner leaflet of the membrane. The perturbation of the membrane combined with the cell wall synthesis inhibition by mutacin 1140 or the combined perturbation of the membrane by mutacin 1140 and kanamycin is attributed to the observed synergy. In order to investigate a mechanism of action for why we were seeing synergy between mutacin 1140 and kanamycin, we set up a bacteria stain treatment using propidium iodide, a red binder of nucleic acids and membrane integrity indicator. Microscopy results (Figure 13, controls Figure 14) showed that chloramphenicol (15  $\mu\text{g}/\text{mL}$ ) is able to inhibit the bactericidal activity of kanamycin (0.5 x MIC). There was a reduction in membrane permeabilization when chloramphenicol was combined with mutacin 1140 and combined with the 0.5 MIC combination of mutacin 1140 and kanamycin. However, this data was not statistically significant. Therefore, we returned to a CFU assay to observe the effect. Figure 15 shows a time lapse comparison between 30 minutes incubation time of the combined and individual dosages of drugs and 24 hours incubation time. In this study, a two-log

increase in colony forming units is observed when chloramphenicol is added to the 0.5 MIC combination of mutacin 1140 and kanamycin. This data does show a protective function of chloramphenicol in this assay. From these results, it does support that the observed synergy is due to the alternate mechanism of action of the aminoglycosides, in that their membrane perturbation in combination with the lipid II binding of mutacin 1140 is the likely cause for the observed synergy. This behavior was also conserved against the methicillin-resistant version of *S. aureus*. Future work that is needed is to determine whether the lantibiotic cell wall inhibition in combination with kanamycin membrane perturbation is the cause for the observed synergy or whether it is the combined membrane disruptive activity causing the synergy. This could be determined by a combination assay featuring vancomycin and kanamycin as well as amoxicillin and kanamycin.

## CHAPTER IV

### DISCUSSION AND CONCLUSIONS

#### **Discussion**

Peptide therapeutics has been a strong source of clinically useful compounds and antibiotics. The previously described data for both mutacin 1140 and occidiofungin support the idea that peptide therapeutics and natural products have the potential for great clinical value. In mutacin 1140, we have a lantibiotic with little resistance which targets a rarely modifiable, essential cell wall biosynthesis component lipid II. In combination with a 4-fold reduced MIC kanamycin mutacin 1140 delivers an 8-fold reduction in MIC, while also killing the bacteria at a faster rate than individually (cell destruction in 1 minute). Because mutacin 1140 resistant mutants have not been identified, the chemistry and structure of 1140 may prove valuable as a template for further development of synthetic antibiotics. Performing rational drug design or reverse target search using lipid II could yield a treasure trove of candidate compounds which by the nature of their target would be slow to acquire resistance. Decades of widespread clinical use of aminoglycosides has strongly reduced their clinical efficacy through the selection of resistant bacteria [100-102]. Having a candidate like mutacin 1140 would allow the resurrection of compounds relegated to second tier status due to resistance or cytotoxic effects and buy time for the antibiotic pipeline to yield new candidate drugs.

The antifungal activity of occidiofungin against a wide array of fungi has been tested. The antifungal activity was observed at micromolar to sub micromolar concentrations. In occidiofungin we have a known antifungal which has a target (actin) which is also a common target for cancer treatment. Work with occidiofungin and the cancer cell lines described in chapter II formed the basis of a United States patent for Occidiofungin formulations and uses thereof (PCT/US2015/049972). Initial acute mouse toxicity study was conducted following subcutaneous and intraperitoneal (i.p.) administration [74]. In this study, we describe a formulation that solubilizes occidiofungin at a concentration that enabled us to evaluate occidiofungin's toxicity following an intravenous route of administration. Furthermore, we evaluated occidiofungin's toxicity against human fibroblast and cancer cells lines. Interestingly, occidiofungin was found to be a potent inhibitor of these cancer cell lines, while there was no significant toxicity observed in mice following a single i.v. dose at 5 mg/kg. This concentration is about seventy-times higher than the concentration that was observed to kill the cancer cells in the *in vitro* toxicity assay. Our current study supports future work aimed at evaluating occidiofungin's potential for treating cancer.

The *in vitro* toxicity in a rat hepatoma (H4IIE) cell line was observed at 5  $\mu\text{M}$ , with a predicted  $\text{TC}_{50}$  value of 3  $\mu\text{M}$  [74]. In this study, the *in vitro* toxicity against a human fibroblast cell line was observed at approximately 1  $\mu\text{M}$ , with a predicted  $\text{TC}_{50}$  value around 0.5  $\mu\text{M}$ . One key difference between these *in vitro* assays is the duration of drug exposure. The exposure time in this study was 48 hours, which is the typical exposure

time for evaluating cancer cell lines [87], while the exposure time against the mouse hepatoma cell line in our initial *in vitro* toxicity assay was only 24 hours [74]. Future studies aimed at evaluated cell viability over a period of time will enable a more complete understanding of the dynamics of cell death in these assays.

In our previous mouse toxicity studies, it was clear that higher doses induced more body weight loss, and this change was dose-responsive [74]. However, body weight loss was not permanent and the mice would regain body weight when dosing ended. Lethargy and ruffled fur were observed in the single i.p. dose experiments on the first and second day after treatment [74]. The loss in body weight in conjunction with decreased thymus weight and the observed increase in neutrophil percentages suggests that occidiofungin causes a non-specific stress response. Activation of the hypothalamic-pituitary-adrenal axis by a non-specific stress response may increase circulating glucocorticoids that can cause apoptosis in developing thymocytes [103]. A loss in body weight was also observed following a 5 mg/kg i.v. administration of occidiofungin. In addition, mild lethargy and some ruffled fur were observed following the i.v. administration of occidiofungin. However, these behavioral changes were not as serious as what was observed following i.p. administration [74]. The mice were responsive and behaved normally by eight hours. There was also an increase in the percentage of neutrophils as observed in the previous study following the i.p. administration of occidiofungin. Future studies aimed at establishing the appropriate dosing regimen along with the administration of Ringers solution will need to be evaluated to determine whether the observed stress response can

be alleviated. No other abnormal behavioral signs were observed. Histological examination of treated mice did not exhibit any signs of organ specific toxicity in our prior study following i.p. and subcutaneous administration [74] and the mice did not exhibit any signs of organ specific toxicity in the current study following i.v. administration. Even at a relatively high dosage of 5 mg/kg, the lack of organ specific toxicity suggests that this compound may have minimal toxic effects and that the observed weight loss may be mitigated in future efficacy studies.

Viability, terminal deoxynucleotidyl transferase dUTP nick end labeling (TUNEL), reactive oxygen species (ROS) detection, membrane and cell wall stability, and membrane mimetic assays were used in a previous study to characterize the effect of occidiofungin on yeast cells [64]. Confocal and electron microscopy experiments were used to visualize morphological changes within treated cells. TUNEL and ROS detection assays revealed an increase in fluorescence with increasing concentrations of the antifungal. Yeast cells appeared to shrink in size and showed the presence of ‘dancing bodies’ at low drug concentrations (1µg/ml). Given that occidiofungin's base molecular weight is 1200 Da, this concentration is around 833 nM. A screen carried out on *Saccharomyces cerevisiae* gene deletion mutants in the apoptotic and autophagy pathways identified the apoptotic gene,  $\Delta yca1$ . Deletion of the *yca1* gene provides a 2-fold increase in resistance. All of the autophagy mutants screened had no difference in sensitivity compared to the wild-type control [64]. Results from previous experiments demonstrate that yeast cells were dying

by an apoptotic mechanism of action. Additional studies are needed to determine whether the human cell lines die by apoptosis following exposure to occidiofungin.

The Mutacin 1140 work done by our lab, in part presented here, represents a valuable opportunity at unlocking a class of novel peptides (lantibiotics) for use in alternative methods. Lantibiotics are both potent and have a broad spectrum of activity which would be invaluable in the clinic. Also, resurrecting other clinical compounds abandoned due to hepatotoxicity, resistance, and availability factors is within reach when combined in synergistic interactions, such as 1140 and kanamycin. Mutacin 1140 is bactericidal against *S. aureus* and has shown itself to be a synergistic partner against both wild type and resistant forms of *S. aureus*. Mutacin 1140, unlike vancomycin, interacts with the N-acetylmuramic sugar (NAM), pyrophosphate, and the first isoprene and the development of resistance due to target modification is unlikely.

Microscopy data suggests that mutacin 1140 killed at a faster rate than vancomycin or kanamycin, and killed more cells over the same period of time compared with any other tested drug individually. CFU count data illustrates that even at sub-MIC concentrations, when combined with kanamycin, mutacin 1140 inhibits *S. aureus* growth over a 24 hour period. We have data showing that there was no synergy observed between mutacin 110 and other non-kanamycin translational inhibitors, as well as a loss of synergy (though still observed activity) when another cell wall inhibitor (nisin) was substituted for mutacin 1140. If the mechanism of action for the observed synergy does not follow the known

MOAs for either compound individually, then perhaps the answer lies in these compounds acting in an alternate mechanism of action. To further study this, we performed a follow up experiment to attempt to assess the action and activity of kanamycin in our cells. Before exposing the cell pellet to kanamycin or mutacin 1140, we preincubated our propidium iodide staining sample pellets with chloramphenicol, an antibiotic which inhibits protein synthesis. It prevents protein chain elongation by inhibiting the peptidyl transferase activity of the bacterial ribosome. Theoretically, we would expect to see an impact on the activity of kanamycin in the presence of chloramphenicol. Our results show that the presence of chloramphenicol causes a marked decrease in kanamycin performance against *S. aureus* (Figure 13). Chloramphenicol also caused a 2 log difference in killing between mutacin 1140, kanamycin, and chloramphenicol in combination versus mutacin 1140 and kanamycin in combination (Figure 15). Our most recent studies revealed a synergistic interaction between vancomycin (a cell wall synthesis inhibitor) and kanamycin (Figure 16). This data in addition to the synergy staining data and the checkerboard data points to our hypothesis that the membrane perturbation of kanamycin and perturbation of cell wall inhibitory activity of mutacin 1140 is working together simultaneously to cause rapid cell death.

In summary, occidiofungin is a natural product produced by the soil bacterium *Burkholderia contaminans* MS14. It was discovered by its ability to inhibit the fungal pathogen of brown patch lawn disease [67]. A soil sample taken from a tuft of green grass surrounded by dead grass has led to the discovery of its potent antifungal activity. In this

study, we have found that occidiofungin also has a potent anticancer activity. Much of the recent focus on drug discovery has been spent on high throughput combinatorial chemistry approaches, which have not yielded the expected number of lead compounds for new chemotherapeutic testing [104]. Nearly half of all natural products used in the clinic have a microbial origin [104]. Our study, along with several other studies [104], demonstrates that there is still an enormous opportunity to identify novel natural products that can be further evaluated for their clinical efficacy in treating microbial infections or cancers. Additional studies in natural product discovery along with combinatorial chemistry can further expand the chances of identifying a compound that can save the lives of those in need. As research focuses oscillate, we need to be cautious of neglecting the potential of the microbial cell in drug discovery.

Follow up experiments and future work for both mutacin 1140 and occidiofungin center on moving into an *in vivo* model. Can mutacin 1140 and kanamycin work in synergy against an active murine infection? What are the thresholds of dosages to optimize treatment in combination *in vivo*? It would be interesting to follow up with studies against kanamycin resistant strains. It would also be of interest whether inactive analogs of kanamycin have any improvement in mutacin 1140 activity. Perhaps setting up a mouse model with an indicator cancer strain like non-small cell lung cancer (NSCLC) and small cell lung cancer (SCLC) would be the first step in testing occidiofungin as a cancer therapeutic. Lung cancer is easily quantified in growth and morphology pre and post drug dose.

Overall, mutacin 1140 and occidiofungin are potent candidate compounds that feature alternative MOAs which were previously unreported. Mutacin 1140 possesses the ability to act in synergy with the aminoglycoside kanamycin, while occidiofungin has an alternative treatment characteristic in that it inhibits cancer cell lines. Both of these MOA's have great value clinically, and should be leveraged and utilized to the utmost in drug development. While natural products research is not receiving the funding it once did from the largest pharmaceutical companies, candidates such as 1140 and occidiofungin form a powerful counterargument as to the efficacy, need, and versatility of this class of compounds for future drug studies in the never-ending push for novel antimicrobials.

## REFERENCES

1. CDC. *Antibiotic / Antimicrobial Resistance*. 2017 6/12/17; Available from: <https://www.cdc.gov/drugresistance/index.html>.
2. Cummings, K.L., D.J. Anderson, and K.S. Kaye, *Hand hygiene noncompliance and the cost of hospital-acquired methicillin-resistant Staphylococcus aureus infection*. *Infect Control Hosp Epidemiol*, 2010. **31**(4): p. 357-64.
3. Gopal Rao, G., *Risk factors for the spread of antibiotic-resistant bacteria*. *Drugs*, 1998. **55**(3): p. 323-330.
4. Brandl, K., et al., *Vancomycin-resistant enterococci exploit antibiotic-induced innate immune deficits*. *Nature*, 2008. **455**(7214): p. 804-807.
5. Sievert, D.M., et al., *Antimicrobial-resistant pathogens associated with healthcare-associated infections; summary of data reported to the national healthcare safety network at the Centers for Disease Control and prevention, 2009–2010*. *Infection Control Report #0026; Hospital Epidemiology*, 2015. **34**(1): p. 1-14.
6. Casaroto, E., et al., *Agreement on the prescription of antimicrobial drugs*. *BMC Infectious Diseases*, 2015. **15**: p. 248.
7. Costa, S.S., et al., *Multidrug efflux pumps in Staphylococcus aureus: an update*. *The Open Microbiology Journal*, 2013. **7**: p. 59-71.
8. Howden, B.P., et al., *Reduced vancomycin susceptibility in Staphylococcus aureus, including vancomycin-intermediate and heterogeneous vancomycin-*

- intermediate strains: resistance mechanisms, laboratory detection, and clinical implications*. Clinical Microbiology Reviews, 2010. **23**(1): p. 99-139.
9. Boucher, H.W., et al., *Bad Bugs, No Drugs: No ESKAPE! An update from the Infectious Diseases Society of America*. Clinical Infectious Diseases, 2009. **48**(1): p. 1-12.
  10. Rice, L.B., *Federal funding for the study of antimicrobial resistance in nosocomial pathogens: No ESKAPE*. The Journal of Infectious Diseases, 2008. **197**(8): p. 1079-1081.
  11. Bird, S.T., et al., *Risk of acute kidney injury associated with the use of fluoroquinolones*. Canadian Medical Association Journal, p. 23-33 2013.
  12. Kurahashi, K., *Biosynthesis of peptide antibiotics*, in *Biosynthesis*, J. Corcoran, Editor. 1981, Springer Berlin Heidelberg. p. 325-352.
  13. Hancock, R.E.W. and D.S. Chapple, *Peptide antibiotics*. Antimicrobial Agents and Chemotherapy, 1999. **43**(6): p. 1317-1323.
  14. Kaspar, A.A. and J.M. Reichert, *Future directions for peptide therapeutics development*. Drug Discovery Today, 2013. **18**(17): p. 807-817.
  15. Fosgerau, K. and T. Hoffmann, *Peptide therapeutics: current status and future directions*. Drug Discovery Today, 2015. **20**(1): p. 122-128.
  16. Reddy, K.V.R., R.D. Yedery, and C. Aranha, *Antimicrobial peptides: premises and promises*. International Journal of Antimicrobial Agents, 2004. **24**(6): p. 536-547.

17. Hiemstra, P.S., et al., *Antimicrobial peptides and innate lung defenses: Role in infectious and non-infectious lung diseases and therapeutic applications*. Chest, 2015.
18. Al-Mahrous, M.M. and M. Upton, *Discovery and development of lantibiotics; antimicrobial agents that have significant potential for medical application*. Expert Opinion on Drug Discovery, 2011. **6**(2): p. 155-170.
19. Arnison, P.G., et al., *Ribosomally synthesized and post-translationally modified peptide natural products: overview and recommendations for a universal nomenclature*. Natural product reports, 2013. **30**(1): p. 108-160.
20. Boman, *Gene-encoded peptide antibiotics and the concept of innate immunity: an update review*. Scandinavian Journal of Immunology, 1998. **48**(1): p. 15-25.
21. Denning, D.W., *Echinocandins: a new class of antifungal*. Journal of Antimicrobial Chemotherapy, 2002. **49**(6): p. 889-891.
22. Eisenstein, B.I., J.F.B. Oleson, and R.H. Baltz, *Daptomycin: from the mountain to the clinic, with essential help from Francis Tally, MD*. Clinical Infectious Diseases, 2010. **50**(Supplement\_1): p. S10-S15.
23. Woodworth, J.R., et al., *Single-dose pharmacokinetics and antibacterial activity of daptomycin, a new lipopeptide antibiotic, in healthy volunteers*. Antimicrobial Agents and Chemotherapy, 1992. **36**(2): p. 318-325.
24. Pogliano, J., N. Pogliano, and J.A. Silverman, *Daptomycin-mediated reorganization of membrane architecture causes mislocalization of essential cell division proteins*. Journal of Bacteriology, 2012. **194**(17): p. 4494-4504.

25. Lab, S. *Discovery of novel antimicrobial agents*. 2016 [cited 2017; Description of Lab interests and research]. Available from:  
<http://www.bio.tamu.edu/index.php/faculty/smith/lab/>.
26. Hillman, J.D., et al., *Genetic and biochemical analysis of mutacin 1140, a lantibiotic from Streptococcus mutans*. *Infection and Immunity*, 1998. **66**(6): p. 2743-2749.
27. Clarke, J.K., *On the bacterial factor in the aetiology of dental caries*. *British journal of experimental pathology*, 1924. **5**(3): p. 141-147.
28. Liljemark, W.F. and C. Bloomquist, *Human oral microbial ecology and dental caries and periodontal diseases*. *Critical Reviews in Oral Biology & Medicine*, 1996. **7**(2): p. 180-198.
29. Smith, L., et al., *Elucidation of the antimicrobial mechanism of mutacin 1140*. *Biochemistry*, 2008. **47**(10): p. 3308-3314.
30. Escano, J., et al., *The leader peptide of mutacin 1140 has distinct structural components compared to related class I lantibiotics*. *MicrobiologyOpen*, 2014. **3**(6): p. 961-972.
31. Chen, S., et al., *Site-directed mutations in the lanthipeptide mutacin 1140*. *Applied and Environmental Microbiology*, 2013. **79**(13): p. 4015-4023.
32. Ghobrial, O.G., H. Derendorf, and J.D. Hillman, *Pharmacodynamic activity of the lantibiotic MU1140*. *Int J Antimicrob Agents*, 2009. **33**(1): p. 70-4.
33. Draper, L.A., et al., *Lantibiotic Resistance*. *Microbiology and Molecular Biology Reviews*, 2015. **79**(2): p. 171-191.

34. Smith, L., et al., *Covalent structure of mutacin 1140 and a novel method for the rapid identification of lantibiotics*. *European Journal of Biochemistry*, 2000. **267**(23): p. 6810-6816.
35. Smith, L. and J.D. Hillman, *Therapeutic potential of type A (I) lantibiotics, a group of cationic peptide antibiotics*. *Current opinion in microbiology*, 2008. **11**(5): p. 401-408.
36. Neeti, D., et al., *Optimization of the production of the lantibiotic Mutacin 1140 in Minimal Media*. *Process Biochemistry* (Barking, London, England), 2010. **45**(7): p. 1187-1191.
37. Escano, J., et al., *Biosynthesis and transport of the lantibiotic mutacin 1140 produced by Streptococcus mutans*. *Journal of Bacteriology*, 2015. **197**(7): p. 1173-1184.
38. Smith, L., et al., *Structure and dynamics of the lantibiotic mutacin 1140†*. *Biochemistry*, 2003. **42**(35): p. 10372-10384.
39. Chugunov, A., et al., *Lipid-II forms potential "landing terrain" for lantibiotics in simulated bacterial membrane*. *Scientific Reports*, 2013. **3**: p. 1678.
40. Hasper, H.E., et al., *An alternative bactericidal mechanism of action for lantibiotic peptides that target lipid II*. *Science*, 2006. **313**(5793): p. 1636-1637.
41. Shi, C., et al., *Synergistic interactions of nisin in combination with cinnamaldehyde against Staphylococcus aureus in pasteurized milk*. *Food Control*, 2017. **71**: p. 10-16.

42. Sanla-Ead, N., et al., *Antimicrobial activity of cinnamaldehyde and eugenol and their activity after incorporation into cellulose-based packaging films*. Packaging Technology and Science, 2012. **25**(1): p. 7-17.
43. Zhao, X., et al., *Synergy of a combination of nisin and citric acid against Staphylococcus aureus and Listeria monocytogenes*. Food Additives & Contaminants: Part A, 2017: p. null-null.
44. Vukomanović, M., et al., *Nano-engineering the antimicrobial spectrum of lantibiotics: activity of nisin against gram negative bacteria*. Scientific Reports, 2017. **7**(1): p. 4324.
45. Wang, Y., et al., *Antibiotic-loaded, silver core-embedded mesoporous silica nanovehicles as a synergistic antibacterial agent for the treatment of drug-resistant infections*. Biomaterials, 2016. **101**: p. 207-216.
46. Charlier, C., et al., *Fluconazole for the management of invasive candidiasis: where do we stand after 15 years?* Journal of Antimicrobial Chemotherapy, 2006. **57**(3): p. 384-410.
47. Verweij, P.E., et al., *Azole resistance in Aspergillus fumigatus: a side-effect of environmental fungicide use?* The Lancet Infectious Diseases, 2009. **9**(12): p. 789-795.
48. Bajwa, S.J. and A. Kulshrestha, *Fungal infections in intensive care unit: challenges in diagnosis and management*. Annals of Medical and Health Sciences Research, 2013. **3**(2): p. 238-244.

49. Perlin, D.S., R. Rautemaa-Richardson, and A. Alastruey-Izquierdo, *The global problem of antifungal resistance: prevalence, mechanisms, and management*. The Lancet Infectious Diseases.
50. Sheehan, D.J., C.A. Hitchcock, and C.M. Sibley, *Current and emerging azole antifungal agents*. Clin Microbiol Rev, 1999. **12**(1): p. 40-79.
51. Sugar, A., *The polyene macrolide antifungal drugs*. Antimicrob. Agents Annu. 1987.,p. 135-176 1987.
52. Hector, R.F., *Compounds active against cell walls of medically important fungi*. Clin Microbiol Rev, 1993. **6**(1): p. 1-21.
53. Sanguinetti, M., B. Posteraro, and C. Lass-Flörl, *Antifungal drug resistance among Candida species: mechanisms and clinical impact*. Mycoses, 2015. **58**: p. 2-13.
54. Magill, S.S., et al., *Multistate point-prevalence survey of health care-associated infections*. New England Journal of Medicine, 2014. **370**(13): p. 1198-1208.
55. Gu, G., et al., *Genetic and biochemical map for the biosynthesis of occidiofungin, an antifungal produced by Burkholderia contaminans Strain MS14*. Applied and Environmental Microbiology, 2011. **77**(17): p. 6189-6198.
56. Tan, W., et al., *Nonclinical toxicological evaluation of occidiofungin, a unique glycolipopeptide antifungal*. International Journal of Toxicology, 2012. **31**(4): p. 326-336.
57. Lu, S.-E., et al., *Occidiofungin, a unique antifungal glycopeptide produced by a strain of Burkholderia contaminans*. Biochemistry, 2009. **48**(35): p. 8312-8321.

58. Parke, J.L. and D. Gurian-Sherman, *Diversity of the Burkholderia cepacia complex and implications for risk assessment of biological control strains*. Annu Rev Phytopathol, 2001. **39**: p. 225-58.
59. Chiarini, L., et al., *Burkholderia cepacia complex species: health hazards and biotechnological potential*. Trends Microbiol, 2006. **14**(6): p. 277-86.
60. Lu, S., S. Woolfolk, and J. Caceres, *Isolation and identification of Rhizobacteria antagonistic to plant fungal pathogens*. Phytopathology, 2005. **95**(6).
61. Deng, P., et al., *Comparative genome-wide analysis reveals that Burkholderia contaminans MS14 possesses multiple antimicrobial biosynthesis genes but not major genetic loci required for pathogenesis*. MicrobiologyOpen, 2016. **5**(3): p. 353-369.
62. Ravichandran, A., *Characterization and development of occidiofungin (PhD Dissertation)*, in *Biology*. 2016, Texas A&M University. p. 188.
63. Gu, G., et al., *Genetic and biochemical map for the biosynthesis of occidiofungin, an antifungal produced by Burkholderia contaminans Strain MS14*. Appl Environ Microbiol, 2011. **77**(17): p. 6189-98.
64. Emrick, D., et al., *The antifungal occidiofungin triggers an apoptotic mechanism of cell death in yeast*. Journal of Natural Products, 2013. **76**(5): p. 829-838.
65. Moseley, J.B. and B.L. Goode, *The yeast actin cytoskeleton: from cellular function to biochemical mechanism*. Microbiol Mol Biol Rev, 2006. **70**(3): p. 605-45.

66. Ellis, D., et al., *Occidiofungin's chemical stability and in vitro potency against candida species*. Antimicrob Agents Chemother, 2012. **56**(2): p. 765-769.
67. Gu, G., S. Lu, and N. Wang, *AmbR1 and AmbR2 are two transcriptional regulators essential for the antifungal activity of Burkholderia sp strain MS14*. Phytopathology, 2008. **98**(6): p. S63-S63.
68. Gu, G., et al., *A genetic and biochemical map for the biosynthesis of occidiofungin, an antifungal produced by Burkholderia contaminans strain MS14*. Applied and Environmental Microbiology, 2011. **77**(17): p. 6189-6198.
69. Gu, G., et al., *AmbR1 is a key transcriptional regulator for production of antifungal activity of Burkholderia contaminans strain MS14*. FEMS Microbiology Letters, 2009. **297**(1): p. 54-60.
70. Gu, G.Y., et al., *Biosynthesis of an antifungal oligopeptide in Burkholderia contaminans strain MS14*. Biochemical and Biophysical Research Communications, 2009. **380**(2): p. 328-332.
71. Ravichandran, A., et al., *The presence of two cyclase thioesterases expands the conformational freedom of the cyclic Peptide occidiofungin*. Journal of Natural Products, 2013. **76**(2): p. 150-156.
72. Clancy, C.J., et al., *Characterizing the effects of caspofungin on Candida albicans, Candida parapsilosis, and Candida glabrata isolates by simultaneous time-kill and postantifungal-effect experiments*. Antimicrobial Agents and Chemotherapy, 2006. **50**(7): p. 2569-2572.

73. Ernst, E.J., M.E. Klepser, and M.A. Pfaller, *Postantifungal effects of echinocandin, azole, and polyene antifungal agents against Candida albicans and Cryptococcus neoformans*. *Antimicrobial Agents and Chemotherapy*, 2000. **44**(4): p. 1108-1111.
74. Wei, T., et al., *Pre-clinical toxicological evaluation of occidiofungin, a unique glyco-lipopeptide antifungal*. *International Journal of Toxicology*, 2012. **31**(4): p. 326-336.
75. Luster, M.I., et al., *Risk assessment in immunotoxicology. I. Sensitivity and predictability of immune tests*. *Fundamental and Applied Toxicology: Official Journal of the Society of Toxicology*, 1992. **18**(2): p. 200-210.
76. Loftsson, T. and M.E. Brewster, *Cyclodextrins as functional excipients: methods to enhance complexation efficiency*. *Journal of Pharmaceutical Sciences*, 2012. **101**(9): p. 3019-3032.
77. Germolec, D.R., et al., *The accuracy of extended histopathology to detect immunotoxic chemicals*. *Toxicological Sciences: An Official Journal of the Society of Toxicology*, 2004. **82**(2): p. 504-514.
78. Gabay, C., et al., *Somatic mutations and intraclonal variations in the rearranged V $\kappa$  genes of B-non-Hodgkin's lymphoma cell lines*. *European Journal of Haematology*, 1999. **63**(3): p. 180-191.
79. Hamilton, T.C., R.C. Young, and R.F. Ozols, *Experimental model systems of ovarian cancer: applications to the design and evaluation of new treatment approaches*. *Seminars in Oncology*, 1984. **11**(3): p. 285-298.

80. Wright, W.C., W.P. Daniels, and J. Fogh, *Distinction of seventy-one cultured human tumor cell lines by polymorphic enzyme analysis*. Journal of the National Cancer Institute, 1981. **66**(2): p. 239-247.
81. Roccaro, A.M., et al., *Bortezomib as an antitumor agent*. Current Pharmaceutical Biotechnology, 2006. **7**(6): p. 441-448.
82. Tobinai, K., *Proteasome inhibitor, bortezomib, for myeloma and lymphoma*. International Journal of Clinical Oncology, 2007. **12**(5): p. 318-326.
83. Cavo, M., *Proteasome inhibitor bortezomib for the treatment of multiple myeloma*. Leukemia, 2006. **20**(8): p. 1341-1352.
84. Chauhan, D., et al., *Proteasome inhibitor therapy in multiple myeloma*. Molecular Cancer Therapeutics, 2005. **4**(4): p. 686-692.
85. Anderson, K.C., *Bortezomib therapy for myeloma*. Current Hematology Reports, 2004. **3**(1): p. 65-65.
86. Anderson, K.C., *Targeted therapy of multiple myeloma based upon tumor-microenvironmental interactions*. Experimental Hematology, 2007. **35**(4 Suppl 1): p. 155-162.
87. Adams, J., et al., *Proteasome inhibitors: a novel class of potent and effective antitumor agents*. Cancer Research, 1999. **59**(11): p. 2615-2622.
88. McAuliffe, O., R.P. Ross, and C. Hill, *Lantibiotics: structure, biosynthesis and mode of action*. FEMS Microbiology Reviews, 2001. **25**(3): p. 285.

89. Basak, K. and S.K. Majumdar, *Utilization of Carbon and Nitrogen Sources by Streptomyces kanamyceticus for Kanamycin Production*. Antimicrobial Agents and Chemotherapy, 1973. **4**(1): p. 6-10.
90. Umezawa, H., *Kanamycin: its discovery*. Annals of the New York Academy of Sciences, 1958. **76**(2): p. 20-26.
91. Misumi, M. and N. Tanaka, *Mechanism of inhibition of translocation by kanamycin and viomycin: A comparative study with fusidic acid*. Biochemical and Biophysical Research Communications, 1980. **92**(2): p. 647-654.
92. Pestka, S., [28] *The use of inhibitors in studies of protein synthesis*, in *Methods in Enzymology*. 1974, Academic Press. p. 261-282.
93. Suzuki, Y., et al., *Detection of kanamycin-resistant Mycobacterium tuberculosis by identifying mutations in the 16S rRNA Gene*. Journal of Clinical Microbiology, 1998. **36**(5): p. 1220-1225.
94. Licitra, G., *Etymologia: Staphylococcus*. Emerging Infectious Diseases, 2013. **19**(9): p. 1553-1553.
95. Bhakdi, S. and J. Trantum-Jensen, *Alpha-toxin of Staphylococcus aureus*. Microbiological Reviews, 1991. **55**(4): p. 733-751.
96. Shenoy, N., X. Wu, and T. Witzig, *Protocol modification to determine the cytotoxic potential of drugs using cell viability assays that rely on the reducing property of viable cells*. 2017.

97. Rand, K.H., et al., *Reproducibility of the microdilution checkerboard method for antibiotic synergy*. Antimicrobial Agents and Chemotherapy, 1993. **37**(3): p. 613-615.
98. Geissmann, Q., *OpenCFU, a new free and open-source software to count cell colonies and other circular objects*. PLOS ONE, 2013. **8**(2): p. e54072.
99. Wallberg, F., T. Tenev, and P. Meier, *Time-Lapse Imaging of Cell Death*. Cold Spring Harbor Protocols, 2016. **2016**(3): p. pdb.prot087395.
100. Kotra, L.P., J. Haddad, and S. Mobashery, *Aminoglycosides: perspectives on mechanisms of action and resistance and strategies to counter resistance*. Antimicrobial Agents and Chemotherapy, 2000. **44**(12): p. 3249-3256.
101. Jana, S. and J.K. Deb, *Molecular understanding of aminoglycoside action and resistance*. Applied Microbiology and Biotechnology, 2006. **70**(2): p. 140-150.
102. Chandrika, N.T. and S. Garneau-Tsodikova, *A review of patents (2011-2015) towards combating resistance to and toxicity of aminoglycosides*. MedChemComm, 2016. **7**(1): p. 50-68.
103. Fuchs, B.A. and S.B. Pruetz, *Morphine induces apoptosis in murine thymocytes in vivo but not in vitro: involvement of both opiate and glucocorticoid receptors*. The Journal Of Pharmacology And Experimental Therapeutics, 1993. **266**(1): p. 417-423.
104. Demain, A.L. and P. Vaishnav, *Natural products for cancer chemotherapy*. Microbial Biotechnology 2011 **4**(6): p. 687–699.

## APPENDIX A

### FIGURES

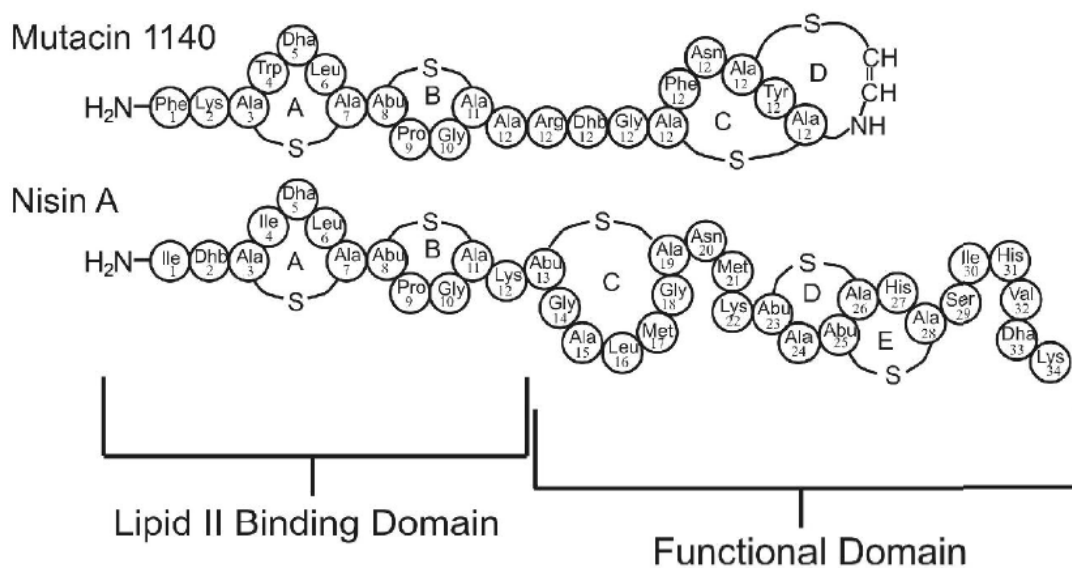


**Figure 1 Mutacin 1140 and Nisin A structure.** (Reprinted from [29])

Lanthionine rings A and B comprise the lipid II binding domain, while the flexible hinge and terminal rings are believed to be important for lateral assembly of membrane complexes. Differences in peptide length are believed to be attributed to ability to form a membrane pore complex.

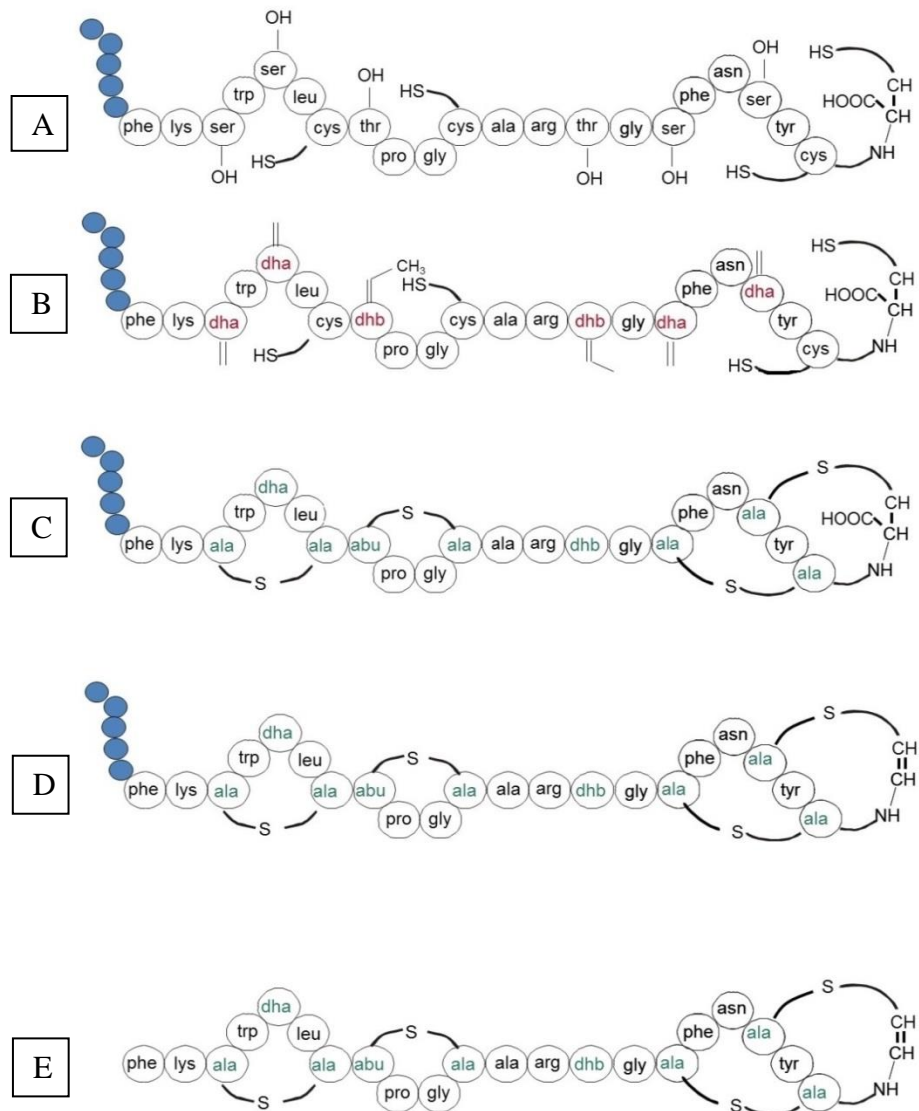


**Figure 2 Mutacin 1140 synthesis.**

2A: Ribosomally synthesized peptide *lanA*. 2B: *lanB* action (dehydratase actor) 2C: *lanC* action (helps facilitate thioether connections and causes cyclization), 2D: *lanD* (decarboxylation action) and 2E: *lanT*, a transporter which allows the movement of the peptide followed by the action of *lanP*, a protease to cleave the leader sequence.

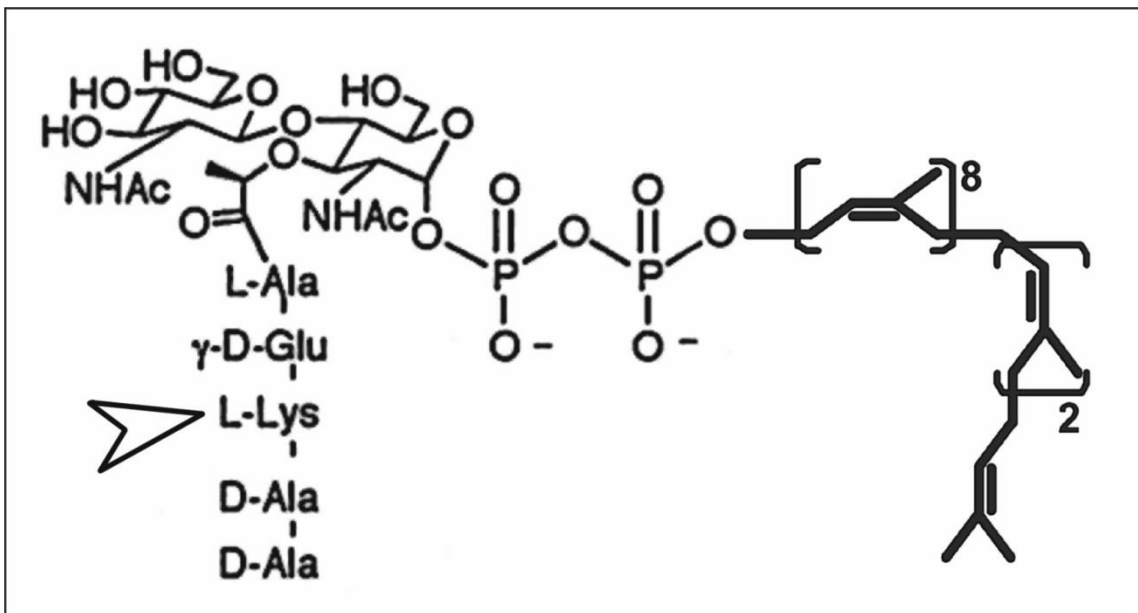
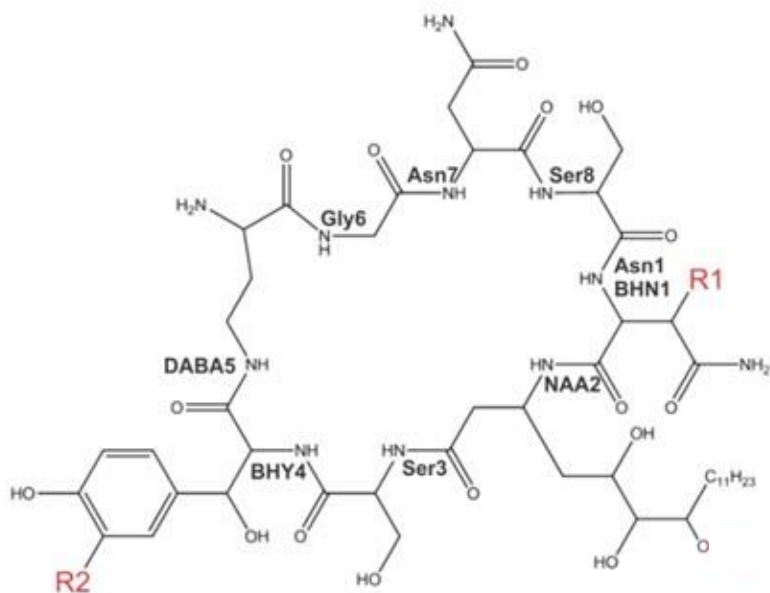


**Figure 3 Structure of lipid II.** (Reprinted from [40])

The triangle represents the site for the nitrobenzoxadiazole (NBD) labeling for microscopy studies. Mutacin 1140 interacts with the first isoprene, NAM, and pyrophosphate via the lanthionine rings A and B.



Covalent Structure of occidiofungin. R1=H or OH; R2=H or Cl;  
R3=Xylose or H.

**Figure 4 Covalent structure of occidiofungin.**

Amino acid positions: Asn/ $\beta$ -hydroxy Asn1, Novel Amino Acid (NAA2), Ser3,  $\beta$ -hydroxy Tyr/chloro  $\beta$ -hydroxy Tyr4, 2,4-diaminobutyric acid (DABA)5, Gly6, Asn7, and Ser8. R1 and R2 represent natural variations in the covalent structure. R1 is either a proton or hydroxyl group and R2 is either a proton or chlorine.

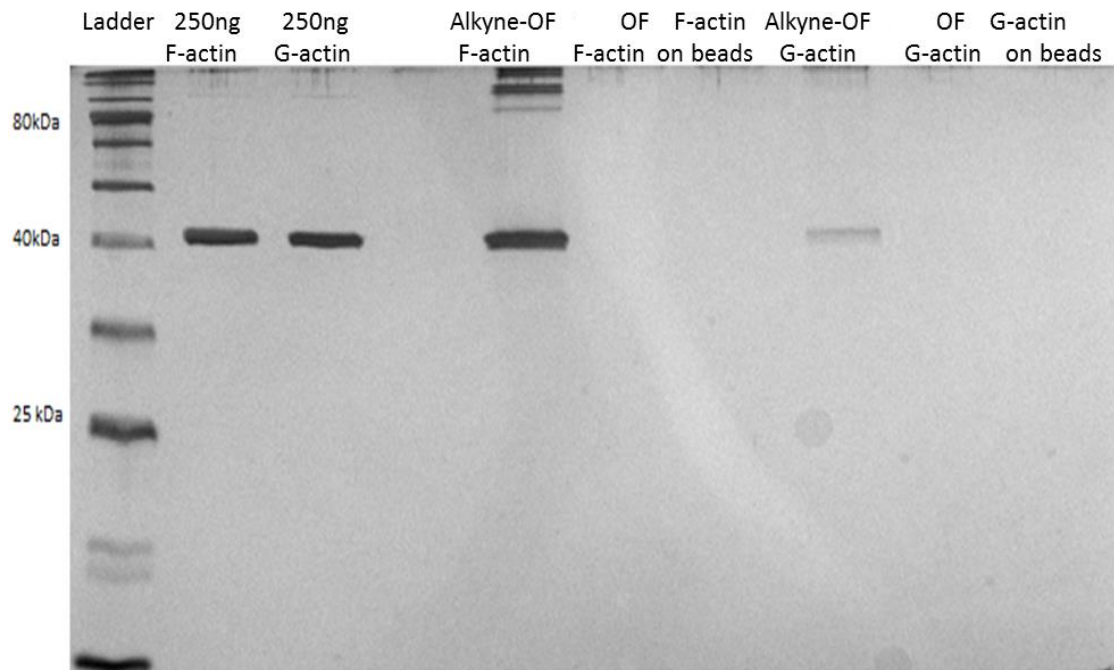


**Figure 5** *In vitro* interaction of occidiofungin with F- and G-actin. (Reprinted with permission from [62])

Affinity pulldown of actin using alkyne-OF: Lane 1-Protein MW ladder, Lane 2-100 ng pure F-actin, Lane 3-100 ng pure G-actin, Lane 4-Empty, Lane 5-F-actin treated with alkyne-OF, Lane 6-F-actin treated with native occidiofungin, Lane 7-F-actin treated with DMSO, Lane 8-G-actin treated with alkyne-OF, Lane 9-G-actin treated with native occidiofungin, Lane 10-G-actin treated with DMSO.

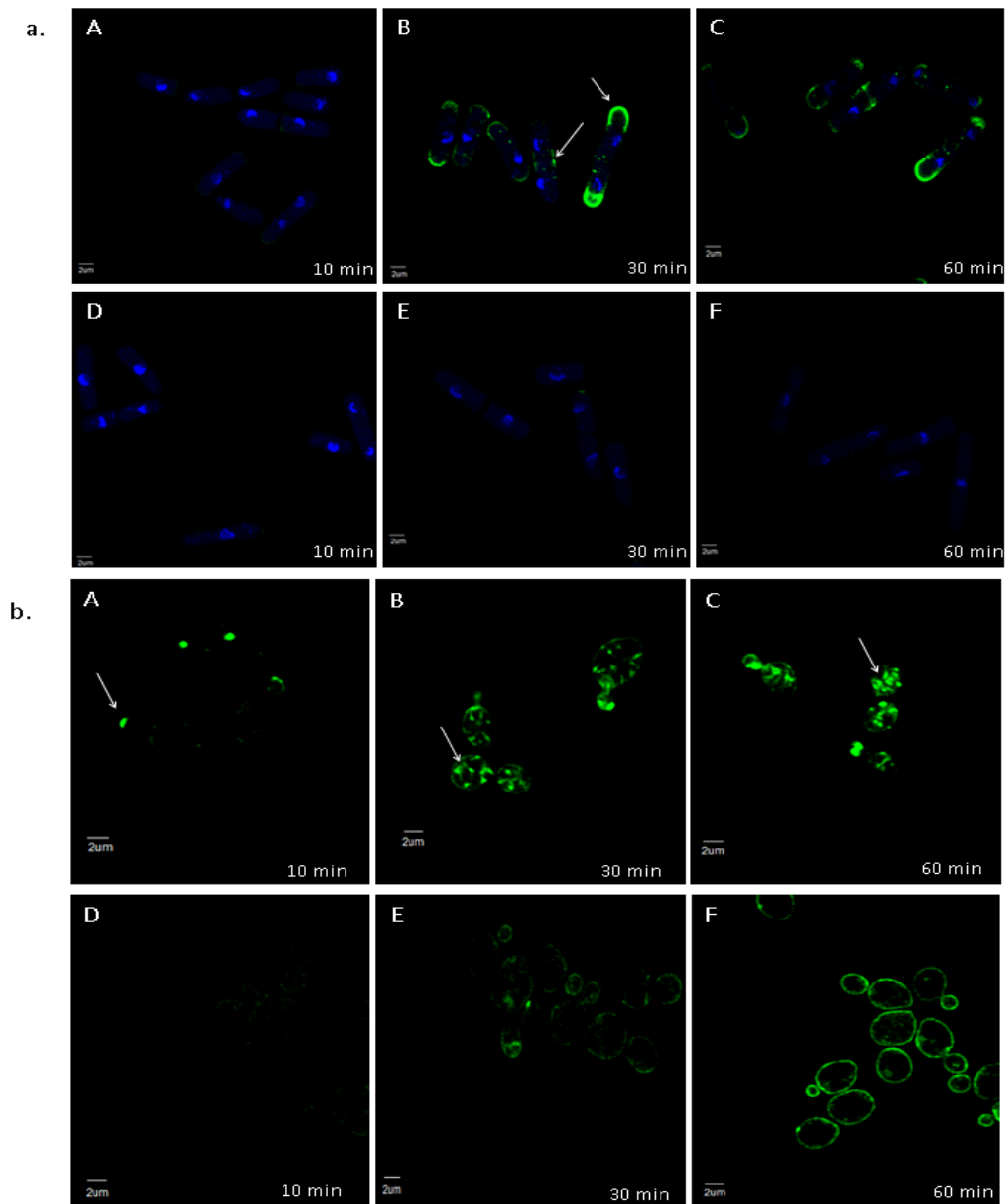


**Figure 6** *In vivo* visualization of occidiofungin. (Reprinted with permission from [62]) Time course analysis (A-C) and competition with native occidiofungin (D-F) in a) *Schizosaccharomyces pombe* and b) *Saccharomyces cerevisiae*. Arrows indicate specific localization patterns observed in each cell at 10, 30, and 60 minutes.

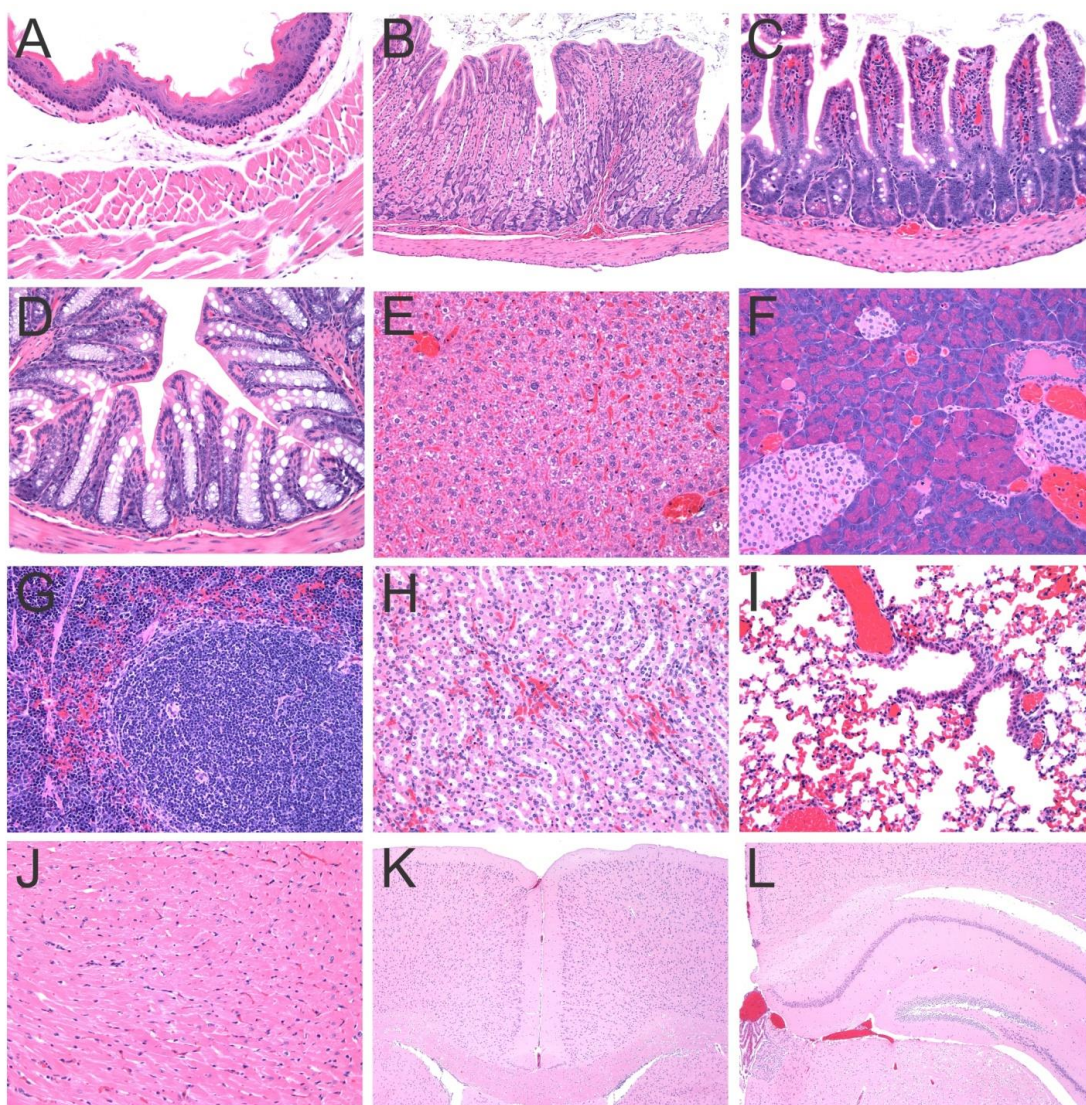


**Figure 7 Occidiofungin mouse histology slides.**

Representative magnifications of histological slides of mice treated with a 5 mg/kg i.v. dose. (A) Esophagus (200X magnification), (B) Stomach (200X magnification), (C) Small Intestine (200X magnification), (D) Colon (200X magnification), (E) Liver (200X magnification), (F) Pancreas (200X magnification), (G) Spleen (200X magnification), (H) Kidney (200X magnification), (I) Lung (200X magnification), (J) Heart (200X magnification), (K) Brain (100X magnification), and (L) Brain (200X magnification). Histological examination was performed on a portion of each organ by using routine paraffin embedding technique and H & E staining. There were no histological abnormalities in the organ tissues of the treated mice in this experiment.

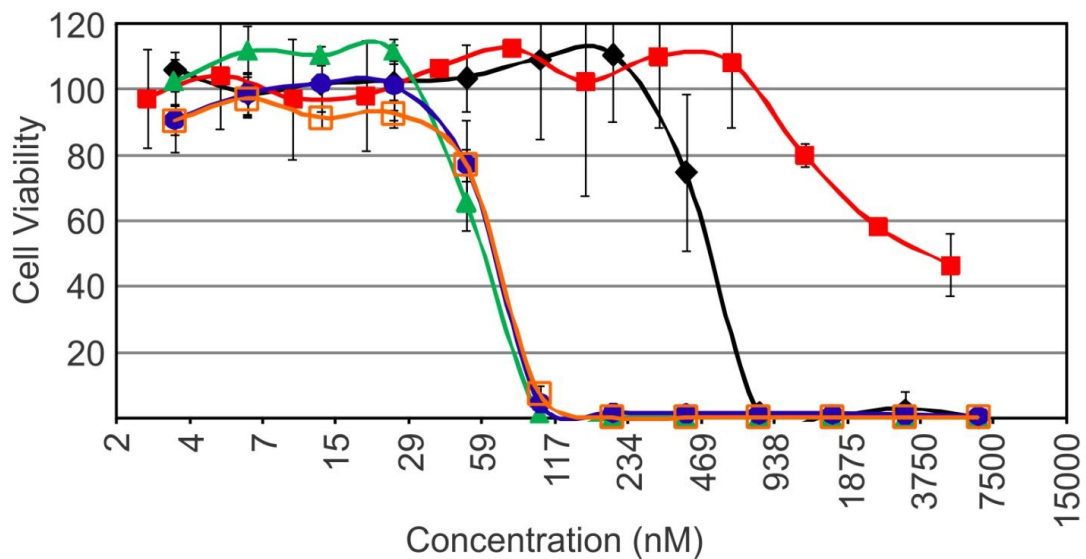
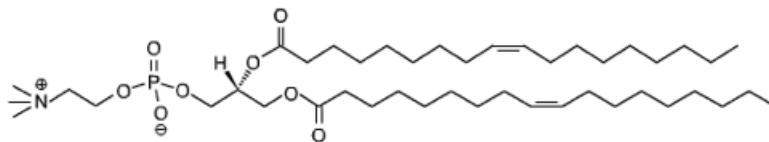


**Figure 8** *In vitro* toxicity screen of occidiofungin.

The TC50 values for occidiofungin against the OVCAR8 (green line and triangles), SW1088 (blue line and circles), and Toledo2631 (orange lines and open squares) cancer cell lines were 61 nM, 68 nM, and 70 nM, respectively. The TC50 value was 533 nM for occidiofungin, while it was 4,091 nM for bortezomib. These values are approximately eight-fold higher than that of the normal human primary dermal fibroblasts cell line tested. Furthermore, the activity against the cancer cell lines was ten to twenty-fold higher than what has been reported against *Candida* species. Results are mean of three independent experiments with one standard deviation.

## DOPC

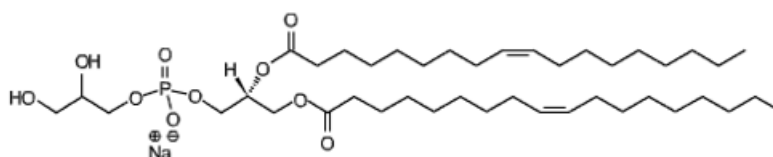
1,2-Dioleoyl-*sn*-Glycero-3-Phosphocholine



©Avanti Polar Lipids

## DOPG

1,2-Dioleoyl-*sn*-Glycero-3-[Phospho-*rac*-(1-glycerol)]



©Avanti Polar Lipids

### Figure 9 Synthetic bilayer membranes. (Reprinted from [29])

Different combinations of DOPC (neutral headgroup) and DOPG (negative charged headgroup) lipids were used to make bilayer vesicles following Avanti Polar Lipids sonication protocol. Vesicles are made in buffered solution containing a self quenching concentration of carboxyfluorescein and separated on a sephadex column to remove free carboxyfluorescein.

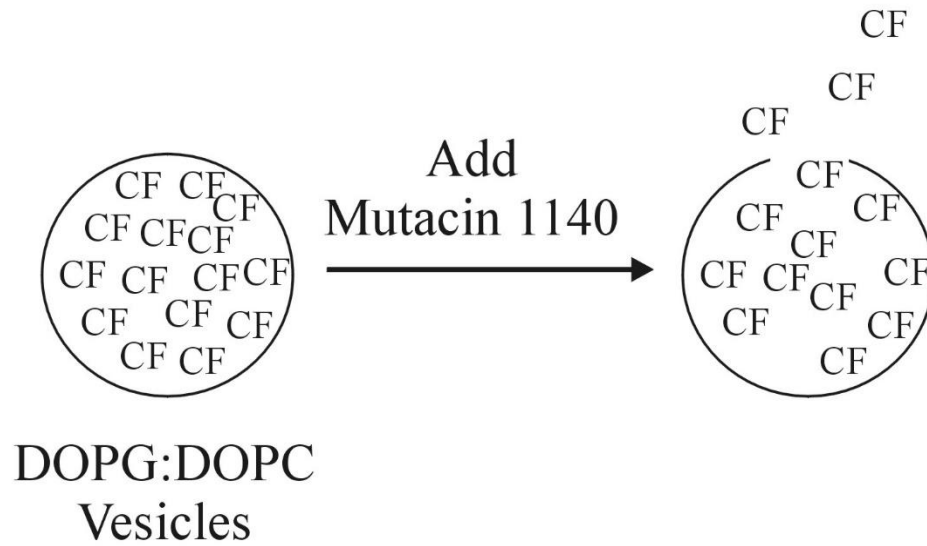
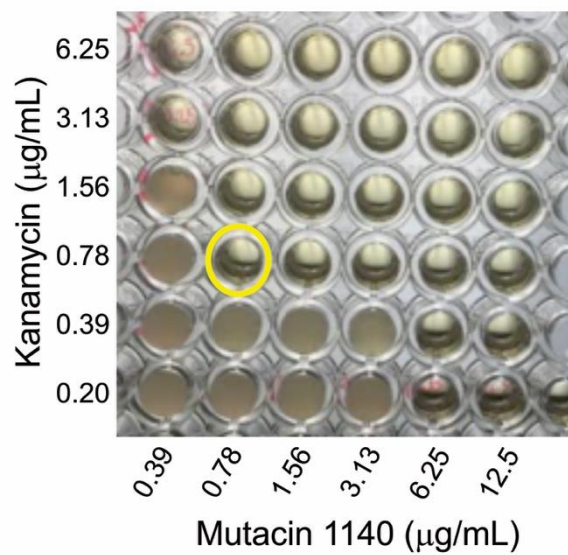


**Figure 10 Measuring the fluorescence intensity of carboxyfluorescein release.**  
(Reprinted from [29])

As mutacin 1140 was introduced to the vesicles, the effect of 1140 caused lysis behavior, releasing the trapped CF. Once free of the vesicle, the CF is detected as it is no longer quenched, signalling that the membrane has been ruptured.



$$\begin{aligned} \varepsilon\text{FIC} &= \text{FIC A} + \text{FIC B} \\ \varepsilon\text{FIC} &= (0.78/6.25) + (0.78/3.13) \\ \varepsilon\text{FIC} &= 0.12 + 0.25 = 0.37 \end{aligned}$$

**Figure 11 Checkerboard microdilution.**

Result for mutacin 1140 combination with kanamycin against *S. aureus*. FIC calculation demonstrates synergy for the combined use of the antibiotics.

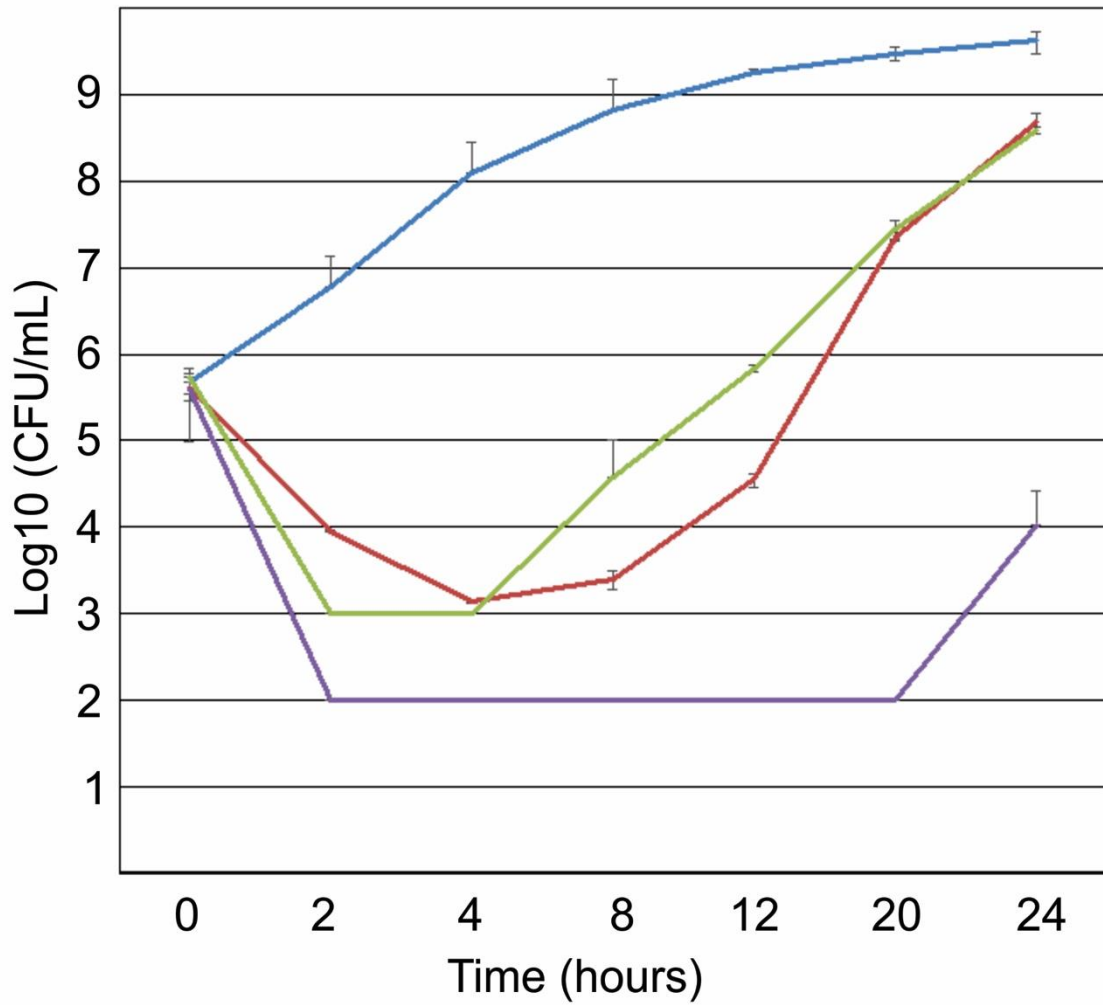


**Figure 12 CFU counts for mutacin 1140 and kanamycin against *S. aureus*.**  
 The blue line represents the no drug control. The red line represents kanamycin individual dosing at .5x MIC. The green line represents .5X MIC dosing for mutacin 1140. The purple line represents the combination dosing of both kanamycin and mutacin 1140.

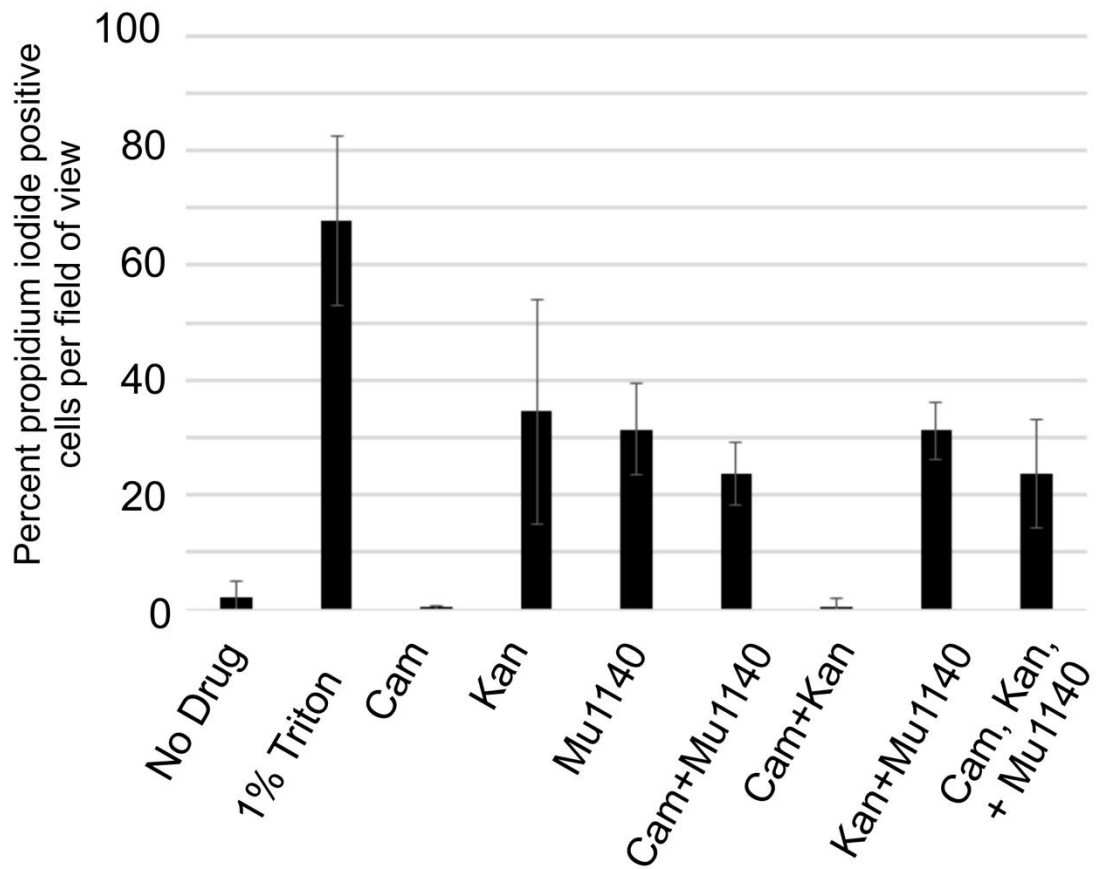


**Figure 13 Propidium iodide staining data, *S. aureus*.**

Percent propidium iodide positive cells per field of view. Chloramphenicol (Cam) inhibits the activity of kanamycin (Kan). One percent Triton served as the positive control. The higher the percent of positive cells, the more cells were red (compromised) in the field of view.

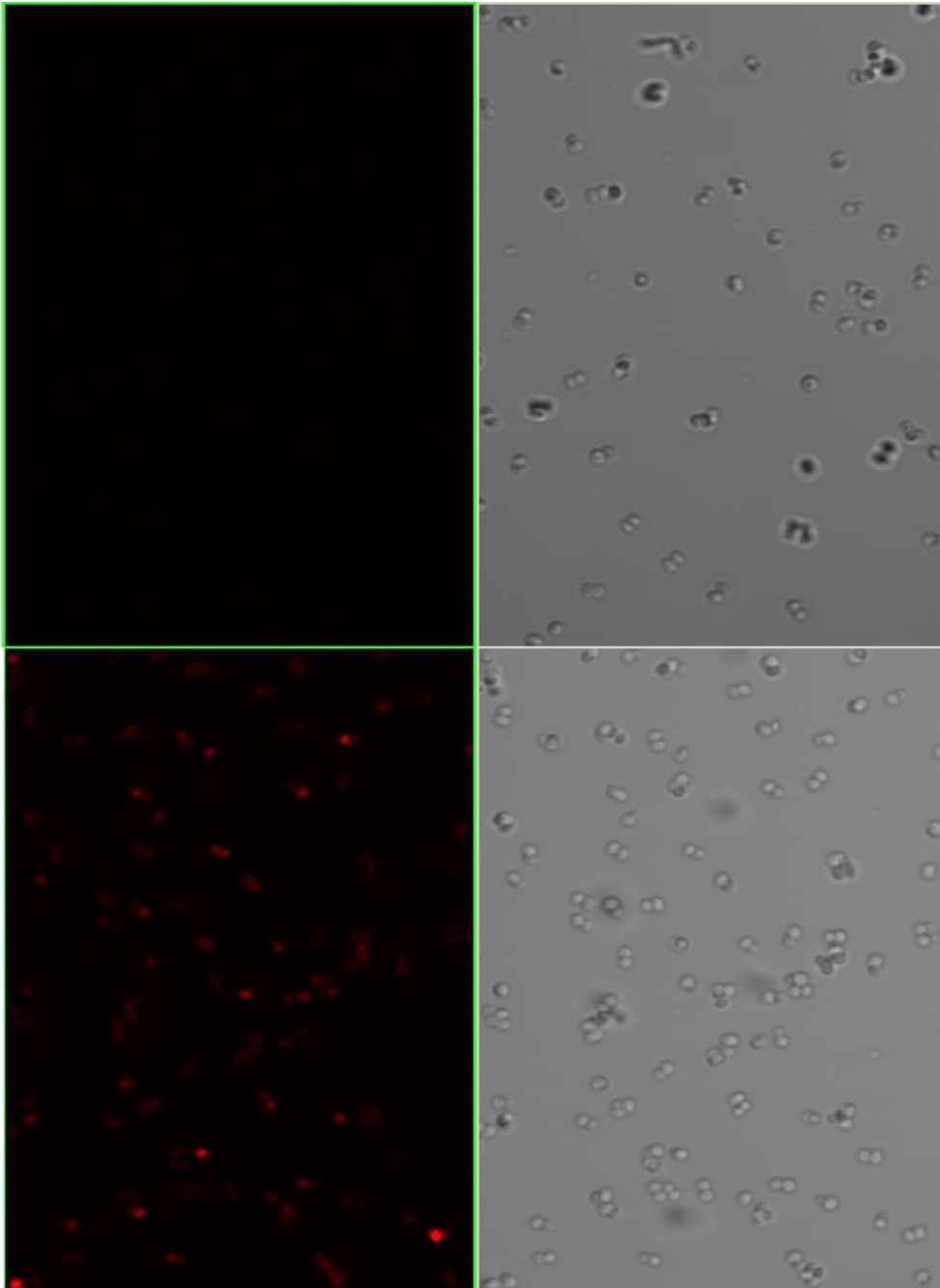


**Figure 14 Propidium iodide staining microscopy positive and negative controls.** The top two panels are the negative controls, no drug present. The lower two panels are the 1% Triton positive controls for membrane permeabilization. The black panels are overlay filters which show the propidium iodide when active.

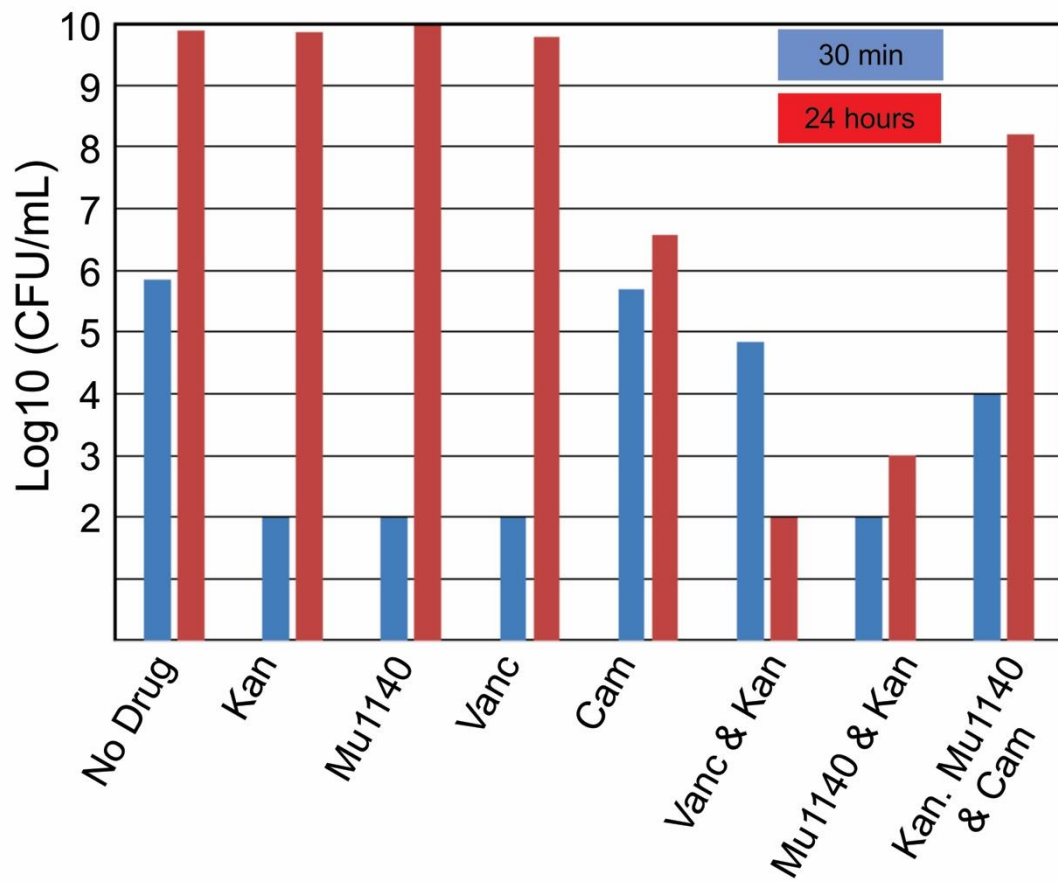


**Figure 15 Viability of *S. aureus* following exposure to antibiotics.**  
 CFU counts were determined at 30 minutes (blue bar) and at 24 hours (red bar).

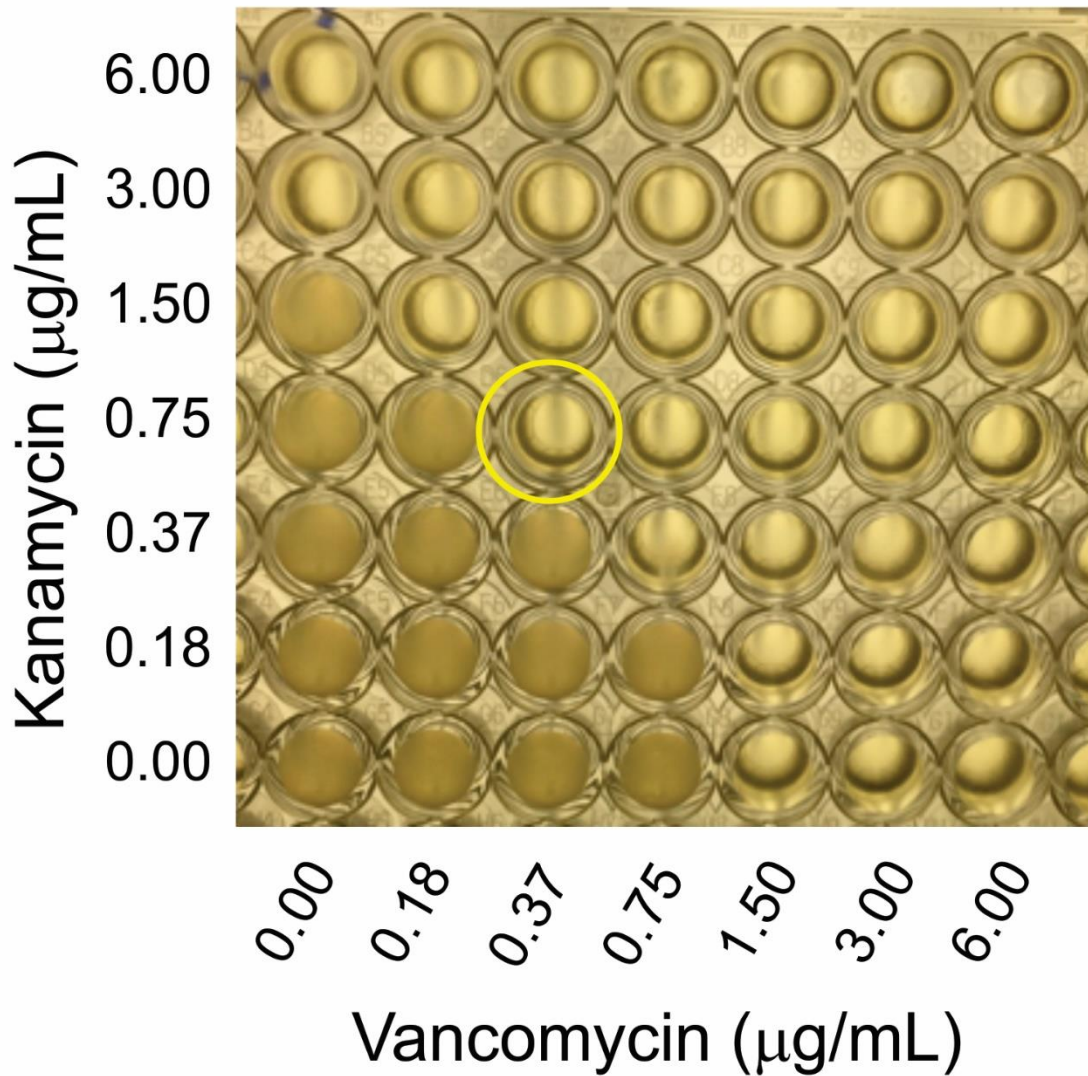


**Figure 16 Checkerboard microdilution assay with vancomycin and kanamycin.** Result for kanamycin in combination with vancomycin against *S. aureus* shows synergy with another lipid II binding antibiotic. FIC calculation demonstrates synergy for the combined use of the antibiotics, noted by yellow circle around example well. Individual MIC values for kanamycin is 3µg/mL and for vancomycin is 1.5µg/mL. FIC values are .25 for kanamycin (0.75µg/3.00µg) and .24 for vancomycin (0.37µg/0.75µg) for a total synergistic value of 0.49, meeting the threshold of <0.5 for synergy.

APPENDIX B

TABLES

**Table 1 Spectrum of activity of occidiofungin**

Strain	Occidiofungin (µg/ml)	Voriconazole (µg/ml)	Fluconazole (µg/ml)	Other susceptible fungi:
<i>Rhizopus spp.</i> <i>Mucor spp.</i> <i>Fusarium spp.</i>	4-8	16 ->16	-	<ul style="list-style-type: none"> <li>• <i>Alternaria alternata</i></li> <li>• <i>Aspergillus fumigatus</i></li> <li>• <i>Geotrichum candidum</i></li> <li>• <i>Macrophomina phaseolina</i></li> <li>• <i>Microsporum gypseum</i></li> <li>• <i>Penicillium spp.</i></li> <li>• <i>Pythium spinosum</i></li> <li>• <i>Pythium ultimum</i></li> <li>• <i>Rhizoctonia solani</i></li> <li>• <i>Trichophyton mentagrophytes</i></li> </ul>
* <i>Candida albicans</i> * <i>Candida krusei</i> * <i>Candida tropicalis</i>	2-4	1-2	-	
# <i>Candida parapsilosis</i>	1-4	-	16->64	
# <i>Cryptococcus neoformans</i>	1-2	-	2-4	

\* -Azole resistant

# - Caspofungin resistant

**Table 2 Percent body weight change, serum chemistry and hematology following administration of drug and excipient control**

	<u>Single IV Dose of</u> <u>Occidiofungin</u>	
	5 mg/kg	0 mg/kg
<b>*Weight Change %</b>	-6.2±9.9	+9.6±1.9
<b>Serum Biochemistry</b>		
Albumin (g/ dl)	3.1±0.6	3.6±0.2
BUN (mg/dl)	29.6±5	24.5±3.3
ALP (U/l)	99±34	116±17
AST (SGOT) U/l	765±692	165±81
*ALT (SGPT) U/l	521±652	36±10
<b>Hematology</b>		
WBC estimate	4750±1225	5830±1550
*Neutrophils %	43±14	16±5
Lymphocytes %	54±15	83±7
Platelet estimate (xK/ul)	39±21	58±58

Animals were sacrificed 24 hours following i.v. administration of occidiofungin. \*Signifies statistically significant differences between treated and control group. p <0.05 was considered statistically significant.

**Table 3 Individual MICs**

Antibiotic MICs	$\mu\text{g/mL}$	$\mu\text{g/mL}$	$\mu\text{g/mL}$	MOA Target
Antibiotic	<i>Staphylococcus aureus</i>	MRSA	<i>Micrococcus luteus</i>	
vancomycin	1	2.5	nd	Lipid II
polymyxin B	>64	>64	>128	Membrane disruption
spectinomycin	50	nd	nd	30S Ribosome
streptomycin	6.25	12.5	6.25	30S Ribosome
gentamycin	5	nd	nd	30S Ribosome
kanamycin	3.25	3.25	nd	30S Ribosome
mutacin 1140	6.25	6.25	0.125	Lipid II
nisin	6.25	6.25	0.625	Lipid II (pore)
tetracycline	12.5	12.5	nd	30S
amoxicillin	3	>240	nd	Peptidoglycan cross linking

**Table 4 Combination MICs**

	$\mu\text{g/mL}$	$\mu\text{g/mL}$
Antibiotic	<i>Staphylococcus aureus</i>	MRSA
nisin/kanamycin	3.125/.8125 (.70)	6.25/2 (2)
nisin/gentamycin	6.25/5(2)	nd
1140/tetracycline	6.25/12.5 (2)	3.125/12.5 (2)
1140/spectinomycin	6.25/50 (2)	nd
1140/vancomycin	6.25/1.25 (2.25)	6.25/2.5 (2)
1140/streptomycin	6.25/6.25 (2)	6.25/12.5 (2)
1140/gentamycin	.195/2.5 (.5312)	nd
1140/kanamycin	.78/.8125 (.3748)	.78/.25 (.3124)

Green numbers mean the combination was synergistic, with 1140/gentamycin borderline synergistic but ultimately falling short of the threshold. Red numbers mean the combination was indifferent in activity. Yellow numbers means the interaction was antagonistic. These numbers are the FIC calculated values. Not detected (nd).